

A Branching Random Walk Method for Many-Body Wigner Quantum Dynamics

Sihong Shao^{1,*} and Yunfeng Xiong¹

¹ *LMAM and School of Mathematical Sciences, Peking University, Beijing 100871, China*

Received 8 June 2018; Accepted (in revised version) 1 July 2018

Abstract. A branching random walk algorithm for many-body Wigner equations and its numerical applications for quantum dynamics in phase space are proposed and analyzed in this paper. Using an auxiliary function, the truncated Wigner equation and its adjoint form are cast into integral formulations, which can be then reformulated into renewal-type equations with probabilistic interpretations. We prove that the first moment of a branching random walk is the solution for the adjoint equation. With the help of the additional degree of freedom offered by the auxiliary function, we are able to produce a weighted-particle implementation of the branching random walk. In contrast to existing signed-particle implementations, this weighted-particle one shows a key capacity of variance reduction by increasing the constant auxiliary function and has no time discretization errors. Several canonical numerical experiments on the 2D Gaussian barrier scattering and a 4D Helium-like system validate our theoretical findings, and demonstrate the accuracy, the efficiency, and thus the computability of the proposed weighted-particle Wigner branching random walk algorithm.

AMS subject classifications: 60J85, 81S30, 45K05, 65M75, 82C10, 81V70, 81Q05

Key words: Wigner equation, branching random walk, quantum dynamics, variance reduction, signed-particle Monte Carlo method, adjoint equation, renewal-type equations, importance sampling, resampling.

1. Introduction

Connection between partial differential equations (PDE) and stochastic processes is an active topic in modern mathematics and provides powerful tools for both probability theory and analysis, especially for PDE of elliptic and parabolic type [1, 2]. In the past few decades, their numerical applications have also burgeoned with a lot of developments, such as the ensemble Monte Carlo method for the Boltzmann transport equation [3–6], the random walk method for the Laplace equation [7] and the diffusion Monte Carlo method for the Schrödinger equation [8, 9]. In particular, the diffusion Monte Carlo method allows

*Corresponding author. *Email addresses:* sihong@math.pku.edu.cn (S. Shao), xiongyf1990@pku.edu.cn (Y. Xiong)

us to go beyond the mean-field approximation and offer a reliable ground state solution to quantum many-body systems. In this work, we focus on the probabilistic approach to the equivalent phase space formalism of quantum mechanics, namely, the Wigner function approach [10], which bears a close analogy to classical mechanics. In recent years, the Wigner equation has been drawing growing attention [11–14] and widely used in nano-electronics [15, 16], non-equilibrium statistical mechanics [17], quantum optics [18], and many-body quantum systems [19]. Actually, a branch of experiment physics in the community of quantum tomography is devoting to reconstructing the Wigner function from measurements [20, 21]. Moreover, the intriguing mathematical structure of the Weyl-Wigner correspondence has also been employed in the deformation quantization [22].

In contrast to its great theoretical advantages, the Wigner equation is extremely difficult to be solved because of the high dimensionality of the phase space as well as the highly oscillating structure of the Wigner function due to the spatial coherence [12, 21]. Although several efficient deterministic solvers, e.g., the conservative spectral element method (SEM) [23] and the third-order advective-spectral-mixed scheme (ASM) [24], have enabled an accurate transient simulation in 2D and 4D phase space, they are still limited by data storage and increasing computational complexity. One possible approach to solving the higher dimensional problems is the Wigner Monte Carlo method, which displays $N^{-\frac{1}{2}}$ convergence (N is the number of samples), regardless of the dimensionality, and scales much better on parallel computing platforms [19, 25].

This work is motivated by a recently developed stochastic method, termed the signed-particle Wigner Monte Carlo method (spWMC) [26–28]. *A particle carrying a signed weight, either -1 or $+1$, is called a signed particle.* This method utilizes the branching of signed particles to capture the quantum coherence, and the numerical accuracy has been validated in 2D situations [29–31]. Very recently, it has been also validated theoretically by exploiting the connection between a piecewise-deterministic Markov process and the weak formulation of the Wigner equation and a random cloud (RC) method was presented [32]¹. In this work, we use an alternative approach to constructing the mathematical framework for spWMC from the viewpoint of computational mathematics, namely, we focus on the probabilistic interpretation of the mild solution of the (truncated) Wigner equation and its adjoint correspondence. In particular, we would like to point out that the resulting stochastic model, the importance sampling and the resampling are three components of a computable scheme for simulating the many-body Wigner quantum dynamics.

Our first objective is to explore the inherent relation between the Wigner equation and a stochastic branching random walk model, as sketched by the diagram below.

$$\boxed{\text{Wigner equation}} \xrightarrow[\gamma(\mathbf{x})]{\text{integral form}} \boxed{\text{Renewal-type equation}} \xleftarrow{\text{moment}} \boxed{\text{Branching random walk}} \quad (1.1)$$

With an auxiliary function $\gamma(\mathbf{x})$, we can cast the Wigner equation (as well as its adjoint equation) into a renewal-type integral equation and prove that its solution is equivalent to

¹We started this work and finished the first version of the manuscript [33] without being aware of the research in [32]. As a consequence, we adopt different mathematical treatments for the Wigner equation and thus propose a different stochastic algorithm the variance of which can be systematically reduced.

the first moment of a stochastic branching random walk. In this manner, we arrive at the stochastic interpretation of the Wigner quantum dynamics, termed the *weighted-particle Wigner branching random walk* (wpWBRW) in this paper. In particular, the wpWBRW method based on the y -truncated Wigner equation (see Section 3.2) may recover the popular spWMC method when a special choice of the auxiliary function is adopted. Here *a particle taking a real-valued weight continuously from -1 to $+1$ is called a weighted particle*. We will demonstrate that wpWBRW with $\gamma(\mathbf{x}) \equiv \gamma_0$ possesses a key capacity of variance reduction by increasing γ_0 and has no time discretization errors.

Although the probabilistic interpretation of the Wigner equation naturally gives rise to a statistical method, in practice we may encounter two major problems. First, such numerical method is point-wise in nature and not very efficient in general unless we are only interested in the solution at specified points [34]. Second, the number of particles in a branching system will grow exponentially in time [35], indicating that the complexity increases dramatically for a long-time simulations. Thus, our second objective is to discuss how to overcome these two obstacles. As for the first, we introduce a dual system of the Wigner equation and derive an equivalent form of an inner product problem, which allows us to draw weighted samples according to the initial Wigner distribution. Besides, by exploiting the principle of importance sampling, we can give a sound interpretation to several fundamental concepts in spWMC, such as particle sign and particle weight. For the second problem, we firstly derive the exact growth rate of branched particles, which behaves like $e^{2M\gamma_0 t}$ in time t , with M pairs of potentials and a constant auxiliary function $\gamma(\mathbf{x}) \equiv \gamma_0$ and then use the idea of resampling to control the particle number within a reasonable size. Roughly speaking, we make a histogram statistic of the weighted particles and resample from it in the next loop. Such a self-consistent scheme allows us to evolve the Wigner quantum dynamics in a time-marching manner and choose appropriate resampling frequencies to control the computational complexity.

The paper is organized as follows. In the rest of this section we will highlight the motivation and significance of the present work as well as the main differences from existing researches in stochastic Wigner simulations. Section 2 reviews briefly the Wigner formalism of quantum mechanics. From both theoretical and numerical aspects, it is more convenient to discuss the truncated Wigner equation, instead of the Wigner equation itself. Thus in Section 3, we illustrate two typical ways to truncate the Wigner equation, termed the k -truncated and the y -truncated models. Section 4 manifests the equivalence between the k -truncated Wigner model and a renewal-type integral equation, where an auxiliary function $\gamma(\mathbf{x})$ is used to introduce a probability measure. In addition, a set of adjoint equation renders an equivalent representation of an inner product problem. In Section 5, we will prove that the first moment of a branching random walk is exactly the solution of the adjoint equation. This probabilistic approach not only validates the branching process treatment, but also allows us to study the mass conservation and exponential growth of particle number, rigorously. After some theoretical analysis, we turn to discuss the importance sampling and the resampling procedure. Section 6 investigates the performance of wpWBRW. The paper is concluded in Section 7 where a discussion on the time discretization issue is detailed.

1.1. Contributions of this paper

Numerical simulations of the Wigner quantum dynamics have attracted considerable attention in the past two decades and different kinds of algorithms emerge probably for different purposes. Whichever kind of numerical scheme one uses, it should offer confidence that the resulting numerical solution must converge to the solution of the same Wigner function (2.7), the sole starting point for any possible numerical discretization. This is the first criterion we should obey in designing a reliable algorithm. However, most existing work on spWMC relies heavily on the numerical results without providing detailed parameter settings, and give only a brief word on the mathematical details about the derivation of the method, except for [26] on the time-independent Wigner equation, and [28] which starts from the semi-discrete model (i.e., the y -truncated version here) instead of Eq. (2.7). Therefore, it is hard for a practician or computational researcher to get a feeling of the whole picture, particularly on when and where the approximation happens and what kind of approximations are applied, which are fundamental issues in evaluating spWMC and must be explicitly stated. The aim of this work is to fill in the gap between the original Wigner function (2.7) and spWMC, and two major contributions are listed below.

- (I) *Build the bridge between the Wigner equation and the branching random walk in a rigorous manner and lay out all related mathematical details step by step, which will give a complete view of the resulting stochastic algorithm.*

Our mathematical framework spans several different branches of mathematics and statistics, some standard terminology from which we borrow to describe the resulting stochastic algorithm, such as renewal-type integral equation, branching random walk, importance sampling, resampling, etc. Definitely, this is not just a change of notations, but using standard mathematical language instead of the pictorial description like ‘creation of particle’, ‘annihilation’. Just because of the rigorous connection, this mathematical description leaves us much more space for further understanding the stochastic algorithm with the help of all existing results and techniques from different branches of mathematics and statistics. Once different numerical schemes have the same starting point, whatever being deterministic or stochastic algorithms, we are able to make a thorough distinction between them. For instance, a highly accurate spectral solver can be used to generate the reference solution for the stochastic one in the accuracy check. Actually, a 4D accuracy check for the stochastic Wigner simulations is performed here for the first time. In addition, a clear and complete mathematical derivation of the stochastic algorithm directly from the original Wigner equation prevents any vague expression in the implementation and thus unfold the ‘blackbox’ of coding wpWBRW.

- (II) *Propose the use of constant auxiliary functions and point out for the first time that the resulting weighted-particle implementation shows a key capacity of variance reduction by increasing the constant auxiliary function and has no time discretization errors in contrast to all existing signed-particle ones.*

As shown in the diagram (1.1), the auxiliary function $\gamma(\mathbf{x})$ is introduced at the first place in our theoretical framework to produce an exponential distribution for branching in time in the renewal-type equation, which exactly plays the role of bridge between the Wigner function and the branching random walk. Our results show that increasing the auxiliary function reduces the variance systematically, which is very important for accurate large-scale simulations. This freedom in choosing the auxiliary function is hidden in the so-called signed-particle implementation. All other existing signed-particle stochastic methods should implicitly adopt a special choice of non-constant $\gamma(\mathbf{x})$ and thus lose the property of variance reduction. This is also the case for the method introduced in [32], though the author also built the connection between a stochastic process and the weak form of the Wigner equation in a different way. More interestingly, accompanied with the chosen constant auxiliary function, the resulting weighted-particle implementation of the Wigner branching random walk has no time discretization errors, which has two consequences (see Section 7 for more details): one is the life-time of particle is analytically calculated; and the other is the branching process is hardly affected by the prescribed time steps.

2. The Wigner equation

In this section, we briefly review the Wigner representation of quantum mechanics. The Wigner function $f(\mathbf{x}, \mathbf{k}, t)$ living in the phase space $(\mathbf{x}, \mathbf{k}) \in \mathbb{R}^{2d}$ for position \mathbf{x} and wavevector \mathbf{k} ,

$$f(\mathbf{x}, \mathbf{k}, t) = \int_{\mathbb{R}^d} d\mathbf{y} e^{-i\mathbf{k}\cdot\mathbf{y}} \rho\left(\mathbf{x} + \frac{\mathbf{y}}{2}, \mathbf{x} - \frac{\mathbf{y}}{2}, t\right) \quad (2.1)$$

is defined by the Weyl-Wigner transform of the density matrix

$$\rho(\mathbf{x}_1, \mathbf{x}_2, t) = \sum_i p_i \Psi_i(\mathbf{x}_1, t) \Psi_i^\dagger(\mathbf{x}_2, t), \quad (2.2)$$

where p_i gives the probability of occupying the i -th state, $2d$ denotes the degree of freedom ($2 \times$ particle number \times dimensionality). Although *it could possibly have negative values*, the Wigner function serves the role as a density function due to the following properties [11, 13]

- $f(\mathbf{x}, \mathbf{k}, t)$ is a real function.
- $\iint_{\mathbb{R}^d \times \mathbb{R}^d} f(\mathbf{x}, \mathbf{k}, t) d\mathbf{x} d\mathbf{k} = 1$.
- The average of a quantum operator \hat{A} can be written in a form

$$\langle \hat{A} \rangle_t = \iint_{\mathbb{R}^d \times \mathbb{R}^d} A(\mathbf{x}, \mathbf{k}) f(\mathbf{x}, \mathbf{k}, t) d\mathbf{x} d\mathbf{k} \quad (2.3)$$

with $A(\mathbf{x}, \mathbf{k})$ the corresponding classical function in phase space.

In particular, we can define the *Wigner (quasi-) probability* W_D on a bounded domain D by taking $A(\mathbf{x}, \mathbf{k}) = \mathbb{1}_D(\mathbf{x}, \mathbf{k})$

$$W_D(t) = \iint_D f(\mathbf{x}, \mathbf{k}, t) d\mathbf{x} d\mathbf{k}. \quad (2.4)$$

To derive the dynamics of the Wigner function, we evaluate its first derivative through the Schrödinger equation (or the quantum Liouville equation)

$$i\hbar \frac{\partial}{\partial t} \Psi_i(\mathbf{x}, t) = -\frac{\hbar^2}{2m} \nabla_{\mathbf{x}}^2 \Psi_i(\mathbf{x}, t) + V(\mathbf{x}, t) \Psi_i(\mathbf{x}, t) \quad (2.5)$$

combine with the Fourier completeness relation

$$\delta(\mathbf{k} - \mathbf{k}') = \frac{1}{(2\pi)^d} \int_{\mathbb{R}^d} d\mathbf{y} e^{i(\mathbf{k}-\mathbf{k}')\cdot\mathbf{y}}, \quad (2.6)$$

and then obtain the Wigner equation

$$\frac{\partial}{\partial t} f(\mathbf{x}, \mathbf{k}, t) + \frac{\hbar\mathbf{k}}{m} \cdot \nabla_{\mathbf{x}} f(\mathbf{x}, \mathbf{k}, t) = \Theta_V[f](\mathbf{x}, \mathbf{k}, t), \quad (2.7)$$

where

$$\Theta_V[f](\mathbf{x}, \mathbf{k}, t) = \int_{\mathbb{R}^d} d\mathbf{k}' f(\mathbf{x}, \mathbf{k}', t) V_W(\mathbf{x}, \mathbf{k} - \mathbf{k}', t), \quad (2.8a)$$

$$V_W(\mathbf{x}, \mathbf{k}, t) = \frac{1}{i\hbar(2\pi)^d} \int_{\mathbb{R}^d} d\mathbf{y} e^{-i\mathbf{k}\cdot\mathbf{y}} D_V(\mathbf{x}, \mathbf{y}, t), \quad (2.8b)$$

$$D_V(\mathbf{x}, \mathbf{y}, t) = V\left(\mathbf{x} + \frac{\mathbf{y}}{2}, t\right) - V\left(\mathbf{x} - \frac{\mathbf{y}}{2}, t\right). \quad (2.8c)$$

Here the nonlocal pseudo-differential term $\Theta_V[f](\mathbf{x}, \mathbf{k}, t)$ contains the quantum information, $D_V(\mathbf{x}, \mathbf{y}, t)$ denotes a central difference of the potential function $V(\mathbf{x}, t)$, the Wigner kernel $V_W(\mathbf{x}, \mathbf{k}, t)$ is defined through the Fourier transform of $D_V(\mathbf{x}, \mathbf{y}, t)$, \hbar is the reduced Planck constant and m is the particle mass (for simplicity, we assume all particles have the same mass throughout this work). Equivalently, we can first perform the integration in \mathbf{k}' -space and arrive at another way to formulate the pseudo-differential term

$$\Theta_V[f](\mathbf{x}, \mathbf{k}, t) = \frac{1}{i\hbar} \int_{\mathbb{R}^d} d\mathbf{y} D_V(\mathbf{x}, \mathbf{y}, t) \widehat{f}(\mathbf{x}, \mathbf{y}, t) e^{-i\mathbf{k}\cdot\mathbf{y}}, \quad (2.9a)$$

$$\widehat{f}(\mathbf{x}, \mathbf{y}, t) = \frac{1}{(2\pi)^d} \int_{\mathbb{R}^d} d\mathbf{k}' f(\mathbf{x}, \mathbf{k}', t) e^{i\mathbf{k}'\cdot\mathbf{y}} := \mathcal{F}^{-1}[f](\mathbf{x}, \mathbf{y}, t). \quad (2.9b)$$

Actually, $\widehat{f}(\mathbf{x}, \mathbf{y}, t)$ is just another notation for $\rho\left(\mathbf{x} + \frac{\mathbf{y}}{2}, \mathbf{x} - \frac{\mathbf{y}}{2}, t\right)$.

One of the most important properties of the Wigner equation lies in the anti-symmetry of the Wigner kernel

$$V_W(\mathbf{x}, \mathbf{k}, t) = -V_W(\mathbf{x}, -\mathbf{k}, t), \quad (2.10)$$

then a simple calculation yields

$$\int_{\mathbb{R}^d} d\mathbf{k} \int_{\mathbb{R}^d} d\mathbf{k}' f(\mathbf{x}, \mathbf{k}', t) V_W(\mathbf{x}, \mathbf{k} - \mathbf{k}', t) = 0, \quad (2.11)$$

which corresponds to the conservation of the zeroth moment (i.e., total particle number or mass)

$$\frac{d}{dt} \iint_{\mathbb{R}^d \times \mathbb{R}^d} f(\mathbf{x}, \mathbf{k}, t) d\mathbf{x} d\mathbf{k} = 0. \quad (2.12)$$

Although the Wigner equation is completely equivalent to the Schrödinger equation in the full space, we would like to point out that such an equivalence is not necessarily true for the truncated Wigner equation (see, e.g. [36]), since for example the truncation of \mathbf{y} -domain may break the Fourier completeness relation (2.6). Therefore, we must be careful when doing benchmark tests for stochastic Wigner simulations by adopting the Schrödinger wavefunction as the reference [28, 30, 31], because the underlying models may not be the same. This also gives rise to the need for highly accurate deterministic algorithms, such as SEM [23] and ASM [24], which can be used to produce a reliable reference solution [29].

3. The truncated Wigner equation

In order to numerically solve the Wigner equation, we need to discuss the truncated Wigner equation on a bounded domain. It should be noted that the double integrations with respect to \mathbf{k}' and \mathbf{y} in the pseudo-differential operator (see Eq. (2.8a) or (2.9a)) involves the infinite domain due to the Fourier transform, posing a formidable challenge in seeking numerical approximations. Intuitively, an feasible way is either truncating \mathbf{k} -space first or truncating \mathbf{y} -space first, denoted below by the k -truncated and y -truncated models, respectively. It is worth noting that no matter what kind of truncation we choose, the mass conservation (2.12) should be maintained in the resulting model as the physical requirement, which may produce additional constraints.

3.1. The k -truncated Wigner equation

A feasible way to formulate the Wigner equation in a bounded domain is to exploit the decay of the Wigner function when $|\mathbf{k}| \rightarrow \infty$. Thus we only need to evaluate the Wigner function $f(\mathbf{x}, \mathbf{k}, t)$ in a finite domain $\mathcal{X} = [-L_1, L_1] \times [-L_2, L_2] \cdots \times [-L_d, L_d]$ ($L_i > 0$) and a simple nullification can be adopted outside \mathcal{X} , that yields the k -truncated Wigner equation

$$\frac{\partial}{\partial t} f(\mathbf{x}, \mathbf{k}, t) + \frac{\hbar \mathbf{k}}{m} \cdot \nabla_{\mathbf{x}} f(\mathbf{x}, \mathbf{k}, t) = \int_{\mathcal{X}} d\mathbf{k}' f(\mathbf{x}, \mathbf{k}', t) V_W(\mathbf{x}, \mathbf{k} - \mathbf{k}', t). \quad (3.1)$$

Combining with the anti-symmetry of the Wigner kernel Eq. (2.10), it naturally yields that

$$\int_{2\mathcal{K}} V_W(\mathbf{x}, \mathbf{k}, t) d\mathbf{k} = 0, \quad (3.2)$$

and thus

$$\frac{d}{dt} \int_{\mathbb{R}^d} \int_{\mathcal{K}} f(\mathbf{x}, \mathbf{k}, t) d\mathbf{x} d\mathbf{k} = 0. \quad (3.3)$$

It should be noted that the domain of integration in Eq. (3.2) must be $2\mathcal{K}$ since $\mathbf{k} - \mathbf{k}' \in 2\mathcal{K}$ in Eq. (3.1) when both \mathbf{k} and \mathbf{k}' belong to \mathcal{K} .

Despite its simplicity, Eq. (3.1) preserves the definition of the Wigner kernel and avoids the artificial periodic extension of D_V as in the y -truncated model (see below). In fact, such formulation paves a rigorous way to connect the deterministic equation with a stochastic process and consequently will be adopted hereafter. In addition, we would like to list two advantages of Eq. (3.1):

- The k -truncated Wigner equation is defined over the continuous \mathbf{k} -space and thus a continuous momentum sampling can be allowed.
- When the Weyl-Wigner transform of $V(\mathbf{x})$ has a close form, we can obtain the explicit formula of the Wigner kernel and avoid the artificial periodic extension of V_W in \mathbf{k} -space.

3.2. The y -truncated Wigner equation

The other way, used in [28], is based on the fact that the inverse Fourier transformed Wigner function $\hat{f}(\mathbf{x}, \mathbf{y}, t)$ defined in Eq. (2.9b) decays when $|\mathbf{y}| \rightarrow \infty$. Thus, we can focus on $\hat{f}(\mathbf{x}, \mathbf{y}, t)$ on a bounded domain $\mathcal{Y} = [-L_1, L_1] \times [-L_2, L_2] \cdots \times [-L_d, L_d] (L_i > 0)$, and define the truncated pseudo-differential operator as

$$\Theta_V^T[f](\mathbf{x}, \mathbf{k}, t) = \frac{1}{i\hbar} \int_{\mathcal{Y}} d\mathbf{y} D_V(\mathbf{x}, \mathbf{y}, t) \hat{f}(\mathbf{x}, \mathbf{y}, t) e^{-i\mathbf{k} \cdot \mathbf{y}}. \quad (3.4)$$

With the assumption that it decays at $y_i > L_i$, we can evaluate $\hat{f}(\mathbf{x}, \mathbf{y}, t)$ at a finite bandwidth through the Poisson summation formula

$$\hat{f}(\mathbf{x}, \mathbf{y}, t) \approx \frac{1}{(2\pi)^d} \sum_{\mathbf{m} \in \mathbb{Z}^d} \left[\left(\prod_{i=1}^d \Delta k_i \right) f(\mathbf{x}, \mathbf{m}\Delta\mathbf{k}, t) e^{i\mathbf{y} \cdot \mathbf{m}\Delta\mathbf{k}} \right], \quad \mathbf{y} \in \mathcal{Y}, \quad (3.5)$$

where $\mathbf{m}\Delta\mathbf{k} = (m_1\Delta k_1, m_2\Delta k_2, \dots, m_d\Delta k_d)$ with Δk_i being the spacing, $m_i \in \mathbb{Z}$, $i = 1, 2, \dots, d$.

Substituting Eq. (3.5) into Eq. (3.4) leads to

$$\Theta_V^T[f](\mathbf{x}, \mathbf{k}, t) \approx \sum_{\mathbf{m} \in \mathbb{Z}^d} f(\mathbf{x}, \mathbf{m}\Delta\mathbf{k}, t) \tilde{V}_W(\mathbf{x}, \mathbf{k} - \mathbf{m}\Delta\mathbf{k}, t), \quad (3.6a)$$

$$\tilde{V}_W(\mathbf{x}, \mathbf{k}, t) = \frac{1}{i\hbar} \frac{1}{|\mathcal{Y}|} \int_{\mathcal{Y}} d\mathbf{y} D_V(\mathbf{x}, \mathbf{y}, t) e^{-i\mathbf{y} \cdot \mathbf{k}}. \quad (3.6b)$$

Here we have let $|\mathcal{Y}| = 2L_1 \times 2L_2 \cdots \times 2L_d$ and used the constraint

$$2L_i \Delta k_i = 2\pi, \quad i = 1, 2, \dots, d, \quad (3.7)$$

which serves as the sufficient and necessary condition to ensure the semi-discrete mass conversation

$$\frac{d}{dt} \int_{\mathbb{R}^d} dx \sum_{\mathbf{n} \in \mathbb{Z}^d} f(\mathbf{x}, \mathbf{n}\Delta\mathbf{k}, t) \Delta\mathbf{k} = 0. \quad (3.8)$$

Suppose the Wigner function at discrete samples $\mathbf{k} = \mathbf{n}\Delta\mathbf{k}$ are wanted, then we immediately arrive at the y -truncated (or semi-discrete) Wigner equation [37–39]

$$\begin{aligned} & \frac{\partial}{\partial t} f(\mathbf{x}, \mathbf{n}\Delta\mathbf{k}, t) + \frac{\hbar \mathbf{n}\Delta\mathbf{k}}{m} \cdot \nabla_{\mathbf{x}} f(\mathbf{x}, \mathbf{n}\Delta\mathbf{k}, t) \\ &= \sum_{\mathbf{m} \in \mathbb{Z}^d} f(\mathbf{x}, \mathbf{m}\Delta\mathbf{k}, t) \tilde{V}_W(\mathbf{x}, \mathbf{n}\Delta\mathbf{k} - \mathbf{m}\Delta\mathbf{k}, t), \end{aligned} \quad (3.9)$$

which indeed provides a straightforward way for stochastic simulations as used in the spWMC method, and possesses the following properties.

- The modified Wigner kernel \tilde{V}_W in Eq. (3.6b) can be treated as the Fourier coefficients of $D_V(\mathbf{x}, \mathbf{y}, t)$ (with a periodic extension), and can be recovered by the inverse Fourier transform (possibly by the inverse fast Fourier transform).
- The continuous convolution is now replaced by a discrete convolution (see Eqs. (2.8a) and (3.6a)), so that sampling from the Wigner kernel can be simply realized in virtue of the cumulative distribution function. However, calculating the cumulative distribution is very time-consuming, especially when the dimension d increases.

Although both truncated models approximate the original problem in some extent, their range of applicability is different. In fact, the modified Wigner potential \tilde{V}_W in y -truncated model is not a trivial approximation to the original Wigner potential (one can refer to the difference between the Fourier coefficients and continuous Fourier transformation). The convergence $\tilde{V}_W \rightarrow V_W$ is only valid when $|\mathcal{Y}| \rightarrow \infty$, or the potential $V(\mathbf{x}, t)$ decays rapidly at the boundary of the finite domain (but this condition is not satisfied for, e.g., the Coulomb-like potential, especially for the Coulomb interaction between two particles). By contrast, the k -truncated model is based on relatively milder assumption, and it is not necessary to change the definition of the Wigner kernel. Thus we would like to stress that *the k -truncated Wigner equation is more appropriate for simulating many-body quantum systems.*

Remark 3.1. The spatial coherence leads to a highly oscillating Wigner function in momentum space [12, 23], which is hard to be captured accurately by any quantized momentum method because of unknown size of the mesh size $\Delta\mathbf{k}$ needed, though there exist many publications starting from the semi-discrete Wigner equation as well as the quantized momentum (see [19] and references therein). That is, it is not an easy task to guarantee a

converged numerical solution to the original Wigner equation (2.7) for the quantized momentum methods. Now we can see that this semi-discrete model is nothing but one type of truncation, i.e., the y -truncated model, and other truncations are also available.

4. Renewal-type integral equations

In order to connect the deterministic partial integro-differential equation (3.1) to a stochastic process, we cast the deterministic equation into a renewal-type integral equation. For this purpose, the first crucial step is to introduce an exponential distribution in its integral formulation via *an auxiliary function* $\gamma(\mathbf{x})$. The second one is to split the Wigner kernel into several positive parts [26], such that each part can be endowed with a probabilistic interpretation. More importantly, to make the resulting branching random walk computable, we derive the adjoint equation of the Wigner equation and obtain an equivalent representation of the inner product (2.3), which explicitly depends on the initial Wigner distribution. Therefore, it provides a much more efficient way to draw samples, and naturally gives rise to several important features of spWMC, such as the particle sign and particle weight.

4.1. Integral formulation with an auxiliary function

The first step is to cast Eq. (3.1) into a renewal-type equation. To this end, we can introduce an auxiliary function $\gamma(\mathbf{x})$ and add the term $\gamma(\mathbf{x})f(\mathbf{x}, \mathbf{k}, t)$ on both sides of Eq. (3.1), yielding

$$\begin{aligned} & \frac{\partial}{\partial t} f(\mathbf{x}, \mathbf{k}, t) + \frac{\hbar \mathbf{k}}{m} \cdot \nabla_{\mathbf{x}} f(\mathbf{x}, \mathbf{k}, t) + \gamma(\mathbf{x}) f(\mathbf{x}, \mathbf{k}, t) \\ &= \int_{\mathcal{K}} d\mathbf{k}' f(\mathbf{x}, \mathbf{k}', t) [V_W(\mathbf{x}, \mathbf{k} - \mathbf{k}', t) + \gamma(\mathbf{x}) \delta(\mathbf{k} - \mathbf{k}')]. \end{aligned} \quad (4.1)$$

At this stage, we only consider a nonnegative bounded $\gamma(\mathbf{x})$, though a time-dependent $\gamma(\mathbf{x}, t)$ can be also introduced if necessary and analyzed in a similar way. In particular, *we strongly recommend the readers to choose a constant* $\gamma(\mathbf{x}) \equiv \gamma_0$ in real applications, for the convenience of both theoretical analysis and numerical computation (vide post). Formally, we can write down its integral formulation through the variation-of-constant formula

$$f(\mathbf{x}, \mathbf{k}, t) = e^{t \cdot \mathcal{A}} f(\mathbf{x}, \mathbf{k}, 0) + \int_0^t e^{(t-t') \cdot \mathcal{A}} [\mathcal{B}(\mathbf{x}, \mathbf{k}, t') + \gamma(\mathbf{x})] f(\mathbf{x}, \mathbf{k}, t') dt', \quad (4.2)$$

where $e^{t \cdot \mathcal{A}}$ denotes the semigroup generated by the operator

$$\mathcal{A} = -\hbar \mathbf{k} / m \cdot \nabla_{\mathbf{x}} - \gamma(\mathbf{x}), \quad (4.3a)$$

$$\mathcal{B}(\mathbf{x}, \mathbf{k}, t) f(\mathbf{x}, \mathbf{k}, t) = \int_{\mathcal{K}} d\mathbf{k}' f(\mathbf{x}, \mathbf{k}', t) V_W(\mathbf{x}, \mathbf{k} - \mathbf{k}', t) \quad (4.3b)$$

is the convolution operator which is assumed to be a bounded operator throughout this work.

When $\gamma(\mathbf{x})$ is bounded, it only imposes a Lyapunov perturbation on a hyperbolic system, so that the operator $e^{t\mathcal{A}}$ is still a C_0 -semigroup [40]. To further determine how the operator $e^{t\mathcal{A}}$ acts on a given function $u(\mathbf{x}, \mathbf{k}, t) \in C^1(L^2(\mathbb{R}^{2d}), [0, T])$, we need to solve the following evolution system

$$\frac{\partial}{\partial t} u(\mathbf{x}, \mathbf{k}, t) + \frac{\hbar \mathbf{k}}{m} \cdot \nabla_{\mathbf{x}} u(\mathbf{x}, \mathbf{k}, t) + \gamma(\mathbf{x}) u(\mathbf{x}, \mathbf{k}, t) = 0, \quad (4.4)$$

the solution of which reads

$$e^{t\mathcal{A}} u(\mathbf{x}, \mathbf{k}, 0) = e^{-\int_0^t \gamma(\mathbf{x}(t-s)) ds} u(\mathbf{x}(t), \mathbf{k}, 0), \quad (4.5)$$

where

$$\mathbf{x}(\Delta t) = \mathbf{x} - \hbar \mathbf{k} \Delta t / m \quad (4.6)$$

is termed the *backward-in-time trajectory* of (\mathbf{x}, \mathbf{k}) with a positive time increment Δt . In fact, Eq. (4.5) can be verified by a simple coordinate conversion

$$\begin{aligned} \frac{\partial u}{\partial t} - \mathcal{A}u = 0 &\xrightarrow{\mathbf{x}'(t) = \mathbf{x} - \frac{\hbar \mathbf{k} t}{m}} \frac{\partial}{\partial t} u(\mathbf{x}'(t), \mathbf{k}, t) = -\gamma(\mathbf{x}'(t), t) u(\mathbf{x}'(t), \mathbf{k}, t) \\ &\xrightarrow{\text{integration in } [t', t]} u(\mathbf{x}'(t), \mathbf{k}, t) = e^{-\int_{t'}^t \gamma(\mathbf{x}'(s)) ds} u(\mathbf{x}'(t'), \mathbf{k}, t') \\ &\xrightarrow{\mathbf{x}'(s) \rightarrow \mathbf{x} - \frac{\hbar \mathbf{k}(t-s)}{m}} u(\mathbf{x}, \mathbf{k}, t) = e^{-\int_{t'}^t \gamma(\mathbf{x}(t-s)) ds} u(\mathbf{x}(t-t'), \mathbf{k}, t'). \end{aligned}$$

After a simple variable substitution ($s + t' \rightarrow s$), the integral formulation of the Wigner equation becomes

$$\begin{aligned} f(\mathbf{x}, \mathbf{k}, t) &= e^{-\int_0^t \gamma(\mathbf{x}(t-s)) ds} f(\mathbf{x}(t), \mathbf{k}, 0) + \int_0^t dt' e^{-\int_{t'}^t \gamma(\mathbf{x}(t-s)) ds} \\ &\quad \times [\mathcal{B}(\mathbf{x}(t-t'), \mathbf{k}, t') + \gamma(\mathbf{x}(t-t'))] f(\mathbf{x}(t-t'), \mathbf{k}, t'). \end{aligned} \quad (4.7)$$

Let

$$\mathcal{H}(t'; \mathbf{x}, t) = \int_{t'}^t \gamma(\mathbf{x}(t-\tau)) e^{-\int_{\tau}^t \gamma(\mathbf{x}(t-s)) ds} d\tau, \quad (4.8)$$

and assume the auxiliary function satisfies

$$\gamma(\mathbf{x}) \geq 0, \quad \lim_{t' \rightarrow -\infty} \int_{t'}^t \gamma(\mathbf{x}(t-s)) ds = +\infty, \quad \forall \mathbf{x} \in \mathbb{R}^d, \quad (4.9)$$

then we have

$$d\mathcal{H}(t'; \mathbf{x}, t) \geq 0, \quad \int_{-\infty}^t d\mathcal{H}(t'; \mathbf{x}, t) = 1 \quad (4.10)$$

implying that $\mathcal{H}(t'; \mathbf{x}, t)$ is a probability measure with respect to t' for a given (\mathbf{x}, t) on $t' \leq t$, characterized by the auxiliary function $\gamma(\mathbf{x})$. Substituting this measure into Eq. (4.7) gives

$$f(\mathbf{x}, \mathbf{k}, t) = [1 - \mathcal{H}(0; \mathbf{x}, t)] f(\mathbf{x}(t), \mathbf{k}, 0) + \int_0^t d\mathcal{H}(t'; \mathbf{x}, t) \int_{\mathcal{K}} d\mathbf{k}' f(\mathbf{x}(t-t'), \mathbf{k}', t') \cdot \left\{ \frac{V_W(\mathbf{x}(t-t'), \mathbf{k} - \mathbf{k}', t')}{\gamma(\mathbf{x}(t-t'))} + \delta(\mathbf{k} - \mathbf{k}') \right\}, \quad (4.11)$$

which can be regarded as a *kind of renewal-type equation* in the renewal theory [35, 41].

Next we turn to consider the Wigner kernel V_W , which cannot be regarded as a transition kernel directly due to possible negative values. Nevertheless, we can regard it as the linear combination of positive semidefinite kernels. In general, the Wigner kernel V_W is composed of M parts

$$V_W = V_{W,1} + V_{W,2} + \cdots + V_{W,M}, \quad (4.12)$$

that corresponds to the potential $V = V_1 + V_2 + \cdots + V_M$, then the Wigner kernel can be split into M pairs

$$V_W = V_W^+ - V_W^-, \quad V_W^\pm = \sum_{m=1}^M V_{W,m}^\pm, \quad (4.13a)$$

$$V_{W,m}^+(\mathbf{x}, \mathbf{k}, t) = \frac{1}{2} |V_{W,m}(\mathbf{x}, \mathbf{k}, t)| + \frac{1}{2} V_{W,m}(\mathbf{x}, \mathbf{k}, t), \quad (4.13b)$$

$$V_{W,m}^-(\mathbf{x}, \mathbf{k}, t) = \frac{1}{2} |V_{W,m}(\mathbf{x}, \mathbf{k}, t)| - \frac{1}{2} V_{W,m}(\mathbf{x}, \mathbf{k}, t). \quad (4.13c)$$

Such a splitting of V_W is rather important in dealing with many-body systems since combining it with the Fourier completeness relation (2.6) helps to reduce the Wigner interaction term (2.8a) into lower dimensional integrals.

Due to the anti-symmetry of V_W (see Eq. (2.10)), it can be easily verified that

$$V_{W,m}^+(\mathbf{x}, \mathbf{k}, t) = V_{W,m}^-(\mathbf{x}, -\mathbf{k}, t). \quad (4.14)$$

Thus, it suffices to define a function Γ on $t \geq t'$, composed of three terms

$$\begin{aligned} & \Gamma(\mathbf{x}(t-t'), \mathbf{k}, t; \mathbf{x}', \mathbf{k}', t') \\ &= V_W^+(\mathbf{x}(t-t'), \mathbf{k} - \mathbf{k}', t') \cdot \delta(\mathbf{x}(t-t') - \mathbf{x}') - V_W^-(\mathbf{x}(t-t'), \mathbf{k} - \mathbf{k}', t') \\ & \quad \cdot \delta(\mathbf{x}(t-t') - \mathbf{x}') + \gamma(\mathbf{x}(t-t')) \cdot \delta(\mathbf{k} - \mathbf{k}') \cdot \delta(\mathbf{x}(t-t') - \mathbf{x}'). \end{aligned} \quad (4.15)$$

Finally, the k -truncated Wigner equation (3.1) can be cast into a Fredholm integral equation of the second kind

$$f(\mathbf{x}, \mathbf{k}, t) = f_0(\mathbf{x}, \mathbf{k}, t) + \mathcal{S}f(\mathbf{x}, \mathbf{k}, t), \quad 0 \leq t \leq T, \quad (4.16)$$

where

$$f_0(\mathbf{x}, \mathbf{k}, t) = e^{-\int_0^t \gamma(\mathbf{x}(t-s)) ds} f(\mathbf{x}(t), \mathbf{k}, 0), \quad (4.17a)$$

$$\mathcal{S}f(\mathbf{x}, \mathbf{k}, t) = \int_0^t dt' \int_{\mathbb{R}^d} d\mathbf{x}' \int_{\mathcal{K}} d\mathbf{k}' K(\mathbf{x}, \mathbf{k}, t; \mathbf{x}', \mathbf{k}', t') f(\mathbf{x}', \mathbf{k}', t'), \quad (4.17b)$$

$$K(\mathbf{x}, \mathbf{k}, t; \mathbf{x}', \mathbf{k}', t') = e^{-\int_{t'}^t \gamma(\mathbf{x}(t-s)) ds} \Gamma(\mathbf{x}(t-t'), \mathbf{k}, t; \mathbf{x}', \mathbf{k}', t'), \quad t \geq t'. \quad (4.17c)$$

Before discussing the probabilistic approach to the integral equation (4.16), we would like first to derive its adjoint equation and attain an equivalent representation of $\langle \hat{A} \rangle_T$, which serves as the cornerstone of wpWBRW.

4.2. Dual system and adjoint equation

In quantum mechanics, it is usually more important to study macroscopically observes $\langle \hat{A} \rangle_t$, such as the averaged position of particles, electron density, etc., than the Wigner function itself. In this regard, we turn to consider the inner product problem

$$\langle g_0, f \rangle = \int_0^T dt \int_{\mathbb{R}^d} d\mathbf{x} \int_{\mathcal{K}} d\mathbf{k} g_0(\mathbf{x}, \mathbf{k}, t) f(\mathbf{x}, \mathbf{k}, t) \quad (4.18)$$

on the domain $\mathbb{R}^d \times \mathcal{K}$ and a finite time interval $[0, T]$. For instance, to evaluate the average value $\langle \hat{A} \rangle_T$ at a given final time T , we should take

$$g_0(\mathbf{x}, \mathbf{k}, t) = A(\mathbf{x}, \mathbf{k}) \delta(t - T), \quad (4.19)$$

then

$$\langle \hat{A} \rangle_T = \langle g_0, f \rangle. \quad (4.20)$$

The main goal of this section is to give the explicit formulation of the adjoint equation, starting from Eqs. (4.16) and (4.19). For brevity, we will assume that the potential is time-independent, and thus the kernels becomes

$$K(\mathbf{x}, \mathbf{k}, t; \mathbf{x}', \mathbf{k}', t') = e^{-\int_{t'}^t \gamma(\mathbf{x}(t-s)) ds} \Gamma(\mathbf{x}(t-t'), \mathbf{k}; \mathbf{x}', \mathbf{k}'), \quad t \geq t', \quad (4.21a)$$

$$\Gamma(\mathbf{x}, \mathbf{k}; \mathbf{x}', \mathbf{k}') = \left[V_W^+(\mathbf{x}, \mathbf{k} - \mathbf{k}') - V_W^-(\mathbf{x}, \mathbf{k} - \mathbf{k}') + \gamma(\mathbf{x}) \delta(\mathbf{k} - \mathbf{k}') \right] \delta(\mathbf{x} - \mathbf{x}'). \quad (4.21b)$$

Suppose the kernel $K(\mathbf{x}, \mathbf{k}, t; \mathbf{x}', \mathbf{k}', t')$ is bounded, then it is easy to verify that \mathcal{S} is a bounded linear operator. Accordingly, we can define the adjoint operator $\mathcal{T} = \mathcal{S}^*$ by

$$\langle g, \mathcal{S}f \rangle = \langle \mathcal{S}^*g, f \rangle = \langle \mathcal{T}g, f \rangle, \quad (4.22)$$

Applying Theorem 4.6 in [42] directly into the Fredholm integral equation of the second kind (4.16) yields

$$\mathcal{T}g(\mathbf{x}', \mathbf{k}', t') = \int_{t'}^T dt \int_{\mathbb{R}^d} d\mathbf{x} \int_{\mathcal{K}} d\mathbf{k} K(\mathbf{x}, \mathbf{k}, t; \mathbf{x}', \mathbf{k}', t') g(\mathbf{x}, \mathbf{k}, t), \quad t \geq t'. \quad (4.23)$$

Formally, it suffices to define

$$g(\mathbf{x}', \mathbf{k}', t') = \mathcal{T}g(\mathbf{x}', \mathbf{k}', t') + g_0(\mathbf{x}', \mathbf{k}', t'), \quad 0 \leq t' \leq T. \quad (4.24)$$

Since

$$\langle g, f \rangle = \langle g, \mathcal{S}f + f_0 \rangle = \langle \mathcal{T}g, f \rangle + \langle g, f_0 \rangle = \langle g, f \rangle - \langle g_0, f \rangle + \langle g, f_0 \rangle, \quad (4.25)$$

we have

$$\langle g_0, f \rangle = \langle g, f_0 \rangle, \quad (4.26)$$

namely

$$\langle \hat{A} \rangle_T = \int_0^T dt' \int_{\mathbb{R}^d} d\mathbf{x}' \int_{\mathcal{X}} d\mathbf{k}' f(\mathbf{x}'(t'), \mathbf{k}', 0) e^{-\int_0^{t'} \gamma(\mathbf{x}'(t'-s)) ds} g(\mathbf{x}', \mathbf{k}', t') \quad (4.27)$$

due to Eq. (4.17a). After performing the coordinate conversion $\mathbf{r}_0 = \mathbf{x}'(t') = \mathbf{x}' - \hbar \mathbf{k}' t' / m$, Eq. (4.27) becomes

$$\langle \hat{A} \rangle_T = \int_0^T dt_0 \int_{\mathbb{R}^d} d\mathbf{r}_0 \int_{\mathcal{X}} d\mathbf{k}_0 f(\mathbf{r}_0, \mathbf{k}_0, 0) e^{-\int_0^{t_0} \gamma(\mathbf{r}_0(s)) ds} g(\mathbf{r}_0(t_0), \mathbf{k}_0, t_0), \quad (4.28)$$

where we have introduced a *forward-in-time trajectory* (in contrast to the backward-in-time trajectory $\mathbf{x}(\Delta t)$ given in Eq. (4.6)) as follows

$$\mathbf{r}_0(\Delta t) = \mathbf{r}_0 + \hbar \mathbf{k}_0 \Delta t / m \quad (4.29)$$

with $\Delta t \geq 0$ being the time increment. Actually, Eq. (4.28) motivates us to combine the exponential factor with g and define a new function $\varphi(\mathbf{r}, \mathbf{k}, t)$ as

$$\varphi(\mathbf{r}, \mathbf{k}, t) = \int_t^T dt' e^{-\int_t^{t'} \gamma(\mathbf{r}(s-t)) ds} g(\mathbf{r}(t'-t), \mathbf{k}, t'). \quad (4.30)$$

Please keep in mind that, it is required $t' \geq t$ for convenience in the definition (4.30), before which $t' \leq t$ is always assumed, for example, see Eq. (4.23). Consequently, from Eq. (4.28), the inner product (4.20) can be determined *only by the 'initial' data*, as stated in the following theorem.

Theorem 4.1 (Representation of inner product). *The average value $\langle \hat{A} \rangle_T$ of a macroscopic quantity $A(\mathbf{x}, \mathbf{k})$ at a given final time T can be evaluated by*

$$\langle \hat{A} \rangle_T = \int_{\mathbb{R}^d} d\mathbf{r} \int_{\mathcal{X}} d\mathbf{k} f(\mathbf{r}, \mathbf{k}, 0) \varphi(\mathbf{r}, \mathbf{k}, 0), \quad (4.31)$$

where φ is defined in Eq. (4.30).

According to Eq. (4.31), in order to evaluate $\langle \hat{A} \rangle_T$, the remaining task is to calculate $\varphi(\mathbf{r}_0, \mathbf{k}_0, 0)$. To this end, we need first to obtain the expression of $g(\mathbf{r}_0(t_0), \mathbf{k}_0, t_0)$ from the dual system (4.24).

Replacing $(\mathbf{x}', \mathbf{k}', t')$ by $(\mathbf{r}_0(t_0), \mathbf{k}_0, t_0)$ and performing the coordinate conversion $\mathbf{x}(t-t') \rightarrow \mathbf{r}_1, \mathbf{k} \rightarrow \mathbf{k}_1, t \rightarrow t_1$ in Eq. (4.24) yield

$$g(\mathbf{r}_0(t_0), \mathbf{k}_0, t_0) = g_0(\mathbf{r}_0(t_0), \mathbf{k}_0, t_0) + \int_{t_0}^T dt_1 \int_{\mathbb{R}^d} d\mathbf{r}_1 \int_{\mathcal{K}} d\mathbf{k}_1 e^{-\int_{t_0}^{t_1} \gamma(\mathbf{r}_1(s-t_0)) ds} \\ \times \Gamma(\mathbf{r}_1, \mathbf{k}_1; \mathbf{r}_0(t_0), \mathbf{k}_0) g(\mathbf{r}_1(t_1 - t_0), \mathbf{k}_1, t_1), \quad (4.32)$$

where the trajectory $\mathbf{r}_1(\Delta t)$ reads

$$\mathbf{r}_1(\Delta t) = \mathbf{r}_1 + \hbar \mathbf{k}_1 \Delta t / m, \quad \Delta t \geq 0, \quad (4.33)$$

which is *not* the same as $\mathbf{r}_0(\Delta t)$ given in Eq. (4.29) due to the disparity in the displacements. By substituting Eq. (4.32) into Eq. (4.28), it yields

$$\langle \hat{A} \rangle_T = \langle \hat{A} \rangle_{T,0} + \int_0^T dt_0 \int_{\mathbb{R}^d} d\mathbf{r}_0 \int_{\mathcal{K}} d\mathbf{k}_0 f(\mathbf{r}_0, \mathbf{k}_0, 0) e^{-\int_0^{t_0} \gamma(\mathbf{r}_0(s)) ds} \int_{t_0}^T dt_1 \int_{\mathbb{R}^d} d\mathbf{r}_1 \\ \cdot \int_{\mathcal{K}} d\mathbf{k}_1 e^{-\int_{t_0}^{t_1} \gamma(\mathbf{r}_1(s-t_0)) ds} \Gamma(\mathbf{r}_1, \mathbf{k}_1; \mathbf{r}_0(t_0), \mathbf{k}_0) g(\mathbf{r}_1(t_1 - t_0), \mathbf{k}_1, t_1), \quad (4.34)$$

where

$$\langle \hat{A} \rangle_{T,0} = \int_{\mathbb{R}^d} d\mathbf{r}_0 \int_{\mathcal{K}} d\mathbf{k}_0 f(\mathbf{r}_0, \mathbf{k}_0, 0) e^{-\int_0^T \gamma(\mathbf{r}_0(s)) ds} A(\mathbf{r}_0(T), \mathbf{k}_0). \quad (4.35)$$

From the dual system (4.24), we can also obtain a similar expression to Eq. (4.32) for $g(\mathbf{r}_1(t_1 - t_0), \mathbf{k}_1, t_1)$, and then corresponding time integration with respect to t_1 in Eq. (4.34) becomes

$$\int_{t_0}^T dt_1 e^{-\int_{t_0}^{t_1} \gamma(\mathbf{r}_1(s-t_0)) ds} g(\mathbf{r}_1(t_1 - t_0), \mathbf{k}_1, t_1) \\ = e^{-\int_{t_0}^T \gamma(\mathbf{r}_1(s-t_0)) ds} A(\mathbf{r}_1(T - t_0), \mathbf{k}_1) + \int_{t_0}^T dt_1 e^{-\int_{t_0}^{t_1} \gamma(\mathbf{r}_1(s-t_0)) ds} \\ \cdot \int_{t_1}^T dt_2 \int_{\mathbb{R}^d} d\mathbf{r}_2 \int_{\mathcal{K}} d\mathbf{k}_2 g(\mathbf{r}_2(t_2 - t_1), \mathbf{k}_2, t_2) \\ \cdot e^{-\int_{t_1}^{t_2} \gamma(\mathbf{r}_2(s-t_1)) ds} \Gamma(\mathbf{r}_2, \mathbf{k}_2; \mathbf{r}_1(t_1 - t_0), \mathbf{k}_1), \quad (4.36)$$

where

$$\mathbf{r}_2(\Delta t) = \mathbf{r}_2 + \hbar \mathbf{k}_2 \Delta t / m, \quad \Delta t \geq 0. \quad (4.37)$$

Combining Eq. (4.36) and the definition (4.30) directly gives the adjoint equation for φ as stated in Theorem 4.2.

Theorem 4.2 (Adjoint equation). *The function $\varphi(\mathbf{r}, \mathbf{k}, t)$ defined in Eq. (4.30) satisfies the following integral equation*

$$\begin{aligned} \varphi(\mathbf{r}, \mathbf{k}, t) &= \mathbb{e}^{-\int_t^T \gamma(\mathbf{r}(s-t))ds} A(\mathbf{r}(T-t), \mathbf{k}) + \int_t^T dt' \int_{\mathbb{R}^d} d\mathbf{r}' \int_{\mathcal{X}} d\mathbf{k}' \varphi(\mathbf{r}', \mathbf{k}', t') \\ &\quad \cdot \mathbb{e}^{-\int_t^{t'} \gamma(\mathbf{r}(s-t))ds} \Gamma(\mathbf{r}', \mathbf{k}'; \mathbf{r}(t'-t), \mathbf{k}). \end{aligned} \quad (4.38)$$

We call Eq. (4.38) the adjoint equation of Eq. (4.7) mainly because $f(\mathbf{r}, \mathbf{k}, 0)$ and $\varphi(\mathbf{r}, \mathbf{k}, 0)$ constitute a dual system in the bilinear form (4.31) (denoted by $\langle \cdot, \cdot \rangle_0$) for determining $\langle \hat{A} \rangle_T$. Combining the formal solution $f(\mathbf{r}, \mathbf{k}, T) = \mathbb{e}^{T(\mathcal{A}+\mathcal{B})} f(\mathbf{r}, \mathbf{k}, 0)$ of the Wigner equation (3.1) as well as Eqs. (2.3) and (4.31) directly yields

$$\begin{aligned} \langle \hat{A} \rangle_T &= \langle f(\mathbf{r}, \mathbf{k}, 0), \varphi(\mathbf{r}, \mathbf{k}, 0) \rangle_0 = \langle f(\mathbf{r}, \mathbf{k}, T), A(\mathbf{r}, \mathbf{k}) \rangle_0 \\ &= \langle \mathbb{e}^{T(\mathcal{A}+\mathcal{B})} f(\mathbf{r}, \mathbf{k}, 0), A(\mathbf{r}, \mathbf{k}) \rangle_0 = \langle f(\mathbf{r}, \mathbf{k}, 0), \mathbb{e}^{-T(\mathcal{A}+\mathcal{B})} A(\mathbf{r}, \mathbf{k}) \rangle_0. \end{aligned} \quad (4.39)$$

As a consequence, we formally obtain $\varphi(\mathbf{r}, \mathbf{k}, 0) = \mathbb{e}^{-T(\mathcal{A}+\mathcal{B})} A(\mathbf{r}, \mathbf{k})$ with $\mathbb{e}^{-T(\mathcal{A}+\mathcal{B})}$ being the adjoint operator of $\mathbb{e}^{T(\mathcal{A}+\mathcal{B})}$, indicating that Eq. (4.38), in some sense, can be treated as an inverse problem of Eq. (4.16), which produces a quantity $\varphi(\mathbf{r}, \mathbf{k}, 0)$ from the observation $A(\mathbf{r}, \mathbf{k})$ at the ending time T .

Moreover, for given (\mathbf{r}, t) on $t' \geq t$, we can similarly introduce a probability measure with respect to t' like

$$\mathcal{G}(t'; \mathbf{r}, t) = \int_t^{t'} \gamma(\mathbf{r}(\tau-t)) \mathbb{e}^{-\int_t^\tau \gamma(\mathbf{r}(s-t))ds} d\tau, \quad (4.40)$$

because of

$$d\mathcal{G}(t'; \mathbf{r}, t) \geq 0, \quad \int_t^{+\infty} d\mathcal{G}(t'; \mathbf{r}, t) = 1 \quad (4.41)$$

under the assumption that the auxiliary function satisfies

$$\forall \mathbf{r} \in \mathbb{R}^d, \quad \gamma(\mathbf{r}) \geq 0, \quad \lim_{t' \rightarrow +\infty} \int_t^{t'} \gamma(\mathbf{r}(t-s))ds = +\infty. \quad (4.42)$$

Substituting the measure (4.40) into Eq. (4.38) also yields a renewal-type equation

$$\begin{aligned} \varphi(\mathbf{r}, \mathbf{k}, t) &= [1 - \mathcal{G}(T; \mathbf{r}, t)] A(\mathbf{r}(T-t), \mathbf{k}) \\ &\quad + \int_t^T d\mathcal{G}(t'; \mathbf{r}, t) \int_{\mathbb{R}^d} d\mathbf{r}' \int_{\mathcal{X}} d\mathbf{k}' \frac{\Gamma(\mathbf{r}', \mathbf{k}'; \mathbf{r}(t'-t), \mathbf{k})}{\gamma(\mathbf{r}(t'-t))} \varphi(\mathbf{r}', \mathbf{k}', t'). \end{aligned} \quad (4.43)$$

life-length τ and carrying a weight w , is marked. The chosen initial data corresponds to those adopted in the renewal-type equation (4.43).

Rule 1 The motion of each particle is described by a right continuous Markov process.

Rule 2 The particle at (\mathbf{r}, \mathbf{k}) dies in the age time interval (t, t') with probability $\mathcal{G}(t'; \mathbf{r}, t)$, which depends on its position \mathbf{r} and the time t (see Eq. (4.40)). In particular, when using the constant auxiliary function $\gamma(\mathbf{r}) \equiv \gamma_0$, the particle dies during time interval (t, t') with probability $1 - e^{-\gamma_0(t'-t)}$, which is totally independent of both its position and age.

Rule 3 If $t + \tau < T$, the particle dies at age $t' = t + \tau$ at state $(\mathbf{r}(\tau), \mathbf{k})$, and produces $2M + 1$ new particles at states $(\mathbf{r}'_{(1)}, \mathbf{k}'_{(1)})$, $(\mathbf{r}'_{(2)}, \mathbf{k}'_{(2)})$, \dots , $(\mathbf{r}'_{(2M+1)}, \mathbf{k}'_{(2M+1)})$, endowed with updated weights $w'_{(1)}$, $w'_{(2)}$, \dots , $w'_{(2M+1)}$, respectively. All these parameters can be determined by the kernel function in Eq. (4.43):

$$\begin{aligned} \frac{\Gamma(\mathbf{r}', \mathbf{k}'; \mathbf{r}(\tau), \mathbf{k})}{\gamma(\mathbf{r}(\tau))} &= \sum_{m=1}^M \frac{\xi_m(\mathbf{r}')}{\gamma(\mathbf{r}(\tau))} \cdot \frac{V_{W,m}^-(\mathbf{r}', \mathbf{k} - \mathbf{k}')}{\xi_m(\mathbf{r}')} \cdot \delta(\mathbf{r}(\tau) - \mathbf{r}') \\ &\quad - \sum_{m=1}^M \frac{\xi_m(\mathbf{r}')}{\gamma(\mathbf{r}(\tau))} \cdot \frac{V_{W,m}^+(\mathbf{r}', \mathbf{k} - \mathbf{k}')}{\xi_m(\mathbf{r}')} \cdot \delta(\mathbf{r}(\tau) - \mathbf{r}') \\ &\quad + 1 \cdot \delta(\mathbf{k} - \mathbf{k}') \cdot \delta(\mathbf{r}(\tau) - \mathbf{r}'), \end{aligned} \quad (5.1)$$

and thus for $1 \leq m \leq M$

$$\mathbf{r}'_{(1)} = \mathbf{r}'_{(2)} = \dots = \mathbf{r}'_{(2M+1)} = \mathbf{r}(\tau), \quad (5.2a)$$

$$\mathbf{k} - \mathbf{k}'_{(2m-1)} \propto \frac{V_{W,m}^-(\mathbf{r}(\tau), \mathbf{k})}{\xi_m(\mathbf{r}(\tau))}, \quad \mathbf{k} - \mathbf{k}'_{(2m)} \propto \frac{V_{W,m}^+(\mathbf{r}(\tau), \mathbf{k})}{\xi_m(\mathbf{r}(\tau))}, \quad (5.2b)$$

$$\mathbf{k}'_{(2M+1)} = \mathbf{k}, \quad (5.2c)$$

$$w'_{(2m-1)} = w \cdot \zeta_{2m-1}(\mathbf{r}(\tau)) \mathbb{1}_{\{\mathbf{k}'_{2m-1} \in \mathcal{X}\}}, \quad (5.2d)$$

$$w'_{(2m)} = w \cdot \zeta_{2m}(\mathbf{r}(\tau)) \mathbb{1}_{\{\mathbf{k}'_{2m} \in \mathcal{X}\}}, \quad w'_{(2M+1)} = w \cdot \zeta_{2M+1}(\mathbf{r}(\tau)) = w, \quad (5.2e)$$

where the function $\xi_m(\mathbf{r})$ is the normalizing function for both $V_{W,m}^+$ and $V_{W,m}^-$, i.e.,

$$\xi_m(\mathbf{r}) = \int_{2\mathcal{X}} V_{W,m}^+(\mathbf{r}, \mathbf{k}) d\mathbf{k} = \int_{2\mathcal{X}} V_{W,m}^-(\mathbf{r}, \mathbf{k}) d\mathbf{k}, \quad (5.3)$$

because of the mass conservation (3.2), and

$$\zeta_{2m-1}(\mathbf{r}) = \frac{\xi_m(\mathbf{r})}{\gamma(\mathbf{r})}, \quad \zeta_{2m}(\mathbf{r}) = -\frac{\xi_m(\mathbf{r})}{\gamma(\mathbf{r})}, \quad \zeta_{2M+1}(\mathbf{r}) = 1. \quad (5.4)$$

Rule 4 If $t + \tau \geq T$, say, the life-length of the particle exceeds $T - t$, so it will migrate to the state $(\mathbf{r}(T - t), \mathbf{k})$ and be frozen. This rule corresponds to the first right-hand-side term of Eq. (4.43), and the related probability is

$$\Pr(\tau \geq T - t) = 1 - \mathcal{G}(T; \mathbf{r}, t) = e^{-\int_t^T \gamma(\mathbf{r}(s-t)) ds}. \quad (5.5)$$

Rule 5 The only interaction between the particles is that the birth time and state of offsprings coincide with the death time and state of their parents.

In spWMC, it is suggested that the Wigner kernel V_W is split into positive and negative parts, namely, $M = 1$, and the auxiliary function is chosen to be the normalizing function $\gamma(\mathbf{r}) \equiv \xi(\mathbf{r})$, resulting in a multiplicative factor $\zeta(\mathbf{r})$ being either $+1$ or -1 according to Eq. (5.4) [27, 28]. This is how we have a signed-particle implementation. Generally, in order to ensure the L^1 -boundedness stated in Theorem 5.1, the bounded weights are required, i.e., $|\zeta_m(\mathbf{r})| \leq 1$, see Eqs. (5.15) and (5.17), and thus the proposed implementation in this work is based on weighted particles, i.e., wpWBRW. In particular, the constant auxiliary function $\gamma(\mathbf{r}) \equiv \gamma_0$ we suggest to use (please refer to Section 7 for more details) should satisfy

$$\gamma_0 \geq \check{\xi} := \max_{1 \leq m \leq 2M+1} \sup_{\mathbf{r} \in \mathbb{R}^d} \xi_m(\mathbf{r}). \quad (5.6)$$

Remark 5.1. Eqs. (5.2b) and (5.3) manifest the importance of the k -truncated model for the Wigner equation because V_W^+ and V_W^- can not be necessarily normalized when $|\mathcal{X}| \rightarrow \infty$. Nevertheless, such a problem can be readily surmounted if only a finite \mathbf{k} -domain \mathcal{X} is taken into account. Notice that one needs to be careful about the domain of integration for the normalizing function $\xi_m(\mathbf{x})$ as $\mathbf{k} - \mathbf{k}' \in 2\mathcal{X}$.

5.2. Stochastic interpretation

In the theory of branching process, all the moments of an age-dependent branching processes satisfy renewal-type integral equations [35], where the term ‘age-dependent’ means the probability that a particle, living at t , dies at $(t, t + \Delta t)$ might not be a constant function of t . In this regard, it suffices to define a stochastic branching Markov process (continuous in time), corresponding to the branching particle system as described earlier.

The random variable of a branching particle system is the family history, a denumerable random sequence corresponding to a unique family tree. First, we need a sequence to identify the objects in a family. Beginning with an ancestor, denoted by $\langle 0 \rangle$, and we can denote its m -th children by $\langle m \rangle$. Similarly, we can denote the j -th child of i -th child by $\langle ij \rangle$, and thus $\langle i_1 i_2 \cdots i_n \rangle$ means i_n -th child of i_{n-1} -th child of \cdots of the i_2 -child of the i_1 -th child, with $i_n \in \{1, 2, \cdots, 2M + 1\}$. The ancestor $\langle 0 \rangle$ is omitted here and hereafter for brevity.

Our branching particle system involves three basic elements: the position \mathbf{r} (or \mathbf{x}), the wavevector \mathbf{k} and the life-length τ , and each particle will either migrate to $\mathbf{r}(\tau) = \mathbf{r} + \hbar \mathbf{k} \tau / m$, then be killed and produce three offsprings, or be frozen when hitting the first

exit time T . Now we can give the definition of a family history, starting from one particle at age t at state (\mathbf{r}, \mathbf{k}) . In the subsequent discussion we let $(\mathbf{r}_0, \mathbf{k}_0) = (\mathbf{r}, \mathbf{k})$.

Definition 5.1. A family history ω stands for a random sequence

$$\omega = ((\tau_0, \mathbf{r}_0, \mathbf{k}_0); (\tau_1, \mathbf{r}_1, \mathbf{k}_1); (\tau_2, \mathbf{r}_2, \mathbf{k}_2); (\tau_3, \mathbf{r}_3, \mathbf{k}_3); (\tau_{11}, \mathbf{r}_{11}, \mathbf{k}_{11}); \cdots), \quad (5.7)$$

where the tuple $(\tau_i, \mathbf{r}_i, \mathbf{k}_i)$ appears in a definite order of enumeration. $\tau_i, \mathbf{r}_i, \mathbf{k}_i$ denote the life-length, starting position and wavevector of the i -th particle, respectively. The exact order of $(\tau_i, \mathbf{r}_i, \mathbf{k}_i)$ is immaterial but is supposed to be fixed. The collection of all family histories is denoted by Ω .

At this stage, the initial time t and the initial state $(\mathbf{r}_0, \mathbf{k}_0)$ of the ancestor particle $\langle 0 \rangle$ are assumed to be non-stochastic. In addition, we denote $Q_i = (\mathbf{r}_i, \mathbf{k}_i)$ and $Q = Q_0 = (\mathbf{r}_0, \mathbf{k}_0) = (\mathbf{r}, \mathbf{k})$ for brevity.

Definition 5.2. For each $\omega = \{(\tau_0, Q); (\tau_1, Q_1); (\tau_2, Q_2); (\tau_3, Q_3); (\tau_{11}, Q_{11}) \cdots\}$, the subfamily ω_i is the family history of $\langle i \rangle$ and its descendants, as defined by

$$\omega_i = \{(\tau_i, Q_i); (\tau_{i1}, Q_{i1}); (\tau_{i2}, Q_{i2}); (\tau_{i3}, Q_{i3}); \cdots\}.$$

The collection of ω_i is denoted by Ω_i .

The following definition characterizes the freezing behavior of the particle.

Definition 5.3. Suppose the family history ω starts at time t and define the arrival time t_i of a branching-and-jump event recursively as

$$t_0 = t, \quad t_{i_1} = t + \tau_0, \quad t_{i_1 i_2 \cdots i_n} = t_{i_1 i_2 \cdots i_{n-1}} + \tau_{i_1 i_2 \cdots i_{n-1}}. \quad (5.8)$$

Then a particle $\langle i_1 i_2 \cdots i_n \rangle$ is said to be frozen at T if the following conditions hold

$$t_{i_1 i_2 \cdots i_n} < T \quad \text{and} \quad t_{i_1 i_2 \cdots i_n} + \tau_{i_1 i_2 \cdots i_n} \geq T. \quad (5.9)$$

In particular, when $t + \tau_0 \geq T$, the ancestor particle $\langle 0 \rangle$ is frozen. Sometimes the particle $\langle i_1 i_2 \cdots i_n \rangle$ is also called alive in the time interval $[t, T]$. The collection of frozen particles is denoted by $\mathcal{E}(\omega)$.

Example 5.1. The family history ω uniquely determines a family history tree, as shown in Fig. 2.

$$\omega = \{(\tau_0, Q_0); (\tau_1, Q_1); (\tau_2, Q_2); (\tau_3, Q_3); (\tau_{21}, Q_{21}); (\tau_{22}, Q_{22}); (\tau_{23}, Q_{23}); (\tau_{231}, Q_{231}); (\tau_{232}, Q_{232}); (\tau_{233}, Q_{233})\}.$$

And ω_2 is a subfamily history describing the family history of Q_2 and its descendants,

$$\omega_2 = \{(\tau_2, Q_2); (\tau_{21}, Q_{21}); (\tau_{22}, Q_{22}); (\tau_{23}, Q_{23}); (\tau_{231}, Q_{231}); (\tau_{232}, Q_{232}); (\tau_{233}, Q_{233})\}.$$

We have $\omega = \{(\tau_0, Q_0); \omega_1; \omega_2; \omega_3\}$. The collection of frozen particles is $\mathcal{E}(\omega) = \{\langle 1 \rangle, \langle 21 \rangle, \langle 22 \rangle, \langle 231 \rangle, \langle 232 \rangle, \langle 233 \rangle, \langle 3 \rangle\}$.

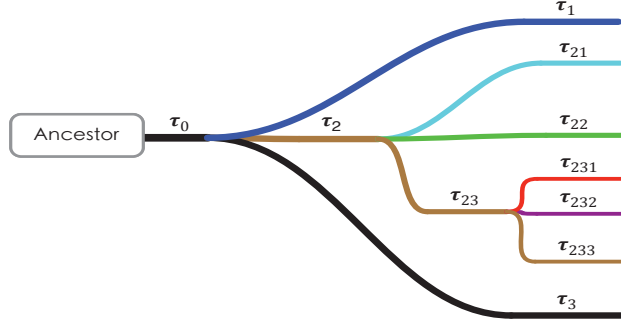


Figure 2: An example of family history tree.

Hereafter, we assume that all particles in the branching particle system will move until reaching the frozen state, and still use Ω to denote the collection of the family history of all frozen particles. Now we need to define a probability measure $\Pi_{Q,t}$ on Ω , corresponding to the branching process started from state $Q = (\mathbf{r}, \mathbf{k})$ at time t .

For the Borel sets $\mathcal{T}_i \subset [0, +\infty)$ ($i = 0, 1, \dots, n$), $\mathcal{R}_i \times \mathcal{K}_i$ ($i = 1, 2, \dots, n$) on Ω , let $E = \{\tau_0 \in T_0, (\tau_{i_1}, Q_{i_1}) \in \mathcal{T}_1 \times \mathcal{R}_1 \times \mathcal{K}_1, \dots, (\tau_{i_1 i_2 \dots i_n}, Q_{i_1 i_2 \dots i_n}) \in \mathcal{T}_n \times \mathcal{R}_n \times \mathcal{K}_n\}$, then the probability of the event E is

$$\begin{aligned}
\Pr(E) &= \int_{\mathcal{T}_0} d\mathcal{G}(t + \tau_0; \mathbf{r}, t) \int_{\mathcal{R}_1} d\mathbf{r}_{i_1} \int_{\mathcal{K}_1} d\mathbf{k}_{i_1} p_{i_1}(\mathbf{r}_{i_1}, \mathbf{k}_{i_1}; \mathbf{r}(\tau_0), \mathbf{k}) \times \dots \\
&\quad \times \int_{\mathcal{T}_{n-1}} d\mathcal{G}(t_{i_1 \dots i_{n-1}} + \tau_{i_1 \dots i_{n-1}}; \mathbf{r}_{i_1 \dots i_{n-1}}, t_{i_1 \dots i_{n-1}}) \\
&\quad \times \int_{\mathcal{R}_n} d\mathbf{r}_{i_1 \dots i_n} \int_{\mathcal{K}_n} d\mathbf{k}_{i_1 \dots i_n} p_{i_n}(\mathbf{r}_{i_1 \dots i_n}, \mathbf{k}_{i_1 \dots i_n}; \mathbf{r}_{i_1 \dots i_{n-1}}(\tau_{i_1 \dots i_{n-1}}), \mathbf{k}_{i_1 \dots i_{n-1}}) \\
&\quad \times \int_{\mathcal{T}_n} d\mathcal{G}(t_{i_1 \dots i_n} + \tau_{i_1 \dots i_n}; \mathbf{r}_{i_1 \dots i_n}, t_{i_1 \dots i_n}) \tag{5.10}
\end{aligned}$$

with $i_l \in \{1, 2, \dots, 2M+1\}$ ($l = 1, 2, \dots, n$). Here $\mathcal{G}(t'; \mathbf{r}, t)$ has been defined in Eq. (4.40) and the transition densities p_{i_l} (for $l = 1, \dots, M$) are given by

$$p_{i_l}(\mathbf{r}, \mathbf{k}; \mathbf{r}', \mathbf{k}') = \begin{cases} \frac{V_{W,m}^-(\mathbf{r}', \mathbf{k} - \mathbf{k}')}{\xi_m(\mathbf{r}')} \cdot \delta(\mathbf{r}' - \mathbf{r}), & i_l = 2m - 1, \\ \frac{V_{W,m}^+(\mathbf{r}', \mathbf{k} - \mathbf{k}')}{\xi_m(\mathbf{r}')} \cdot \delta(\mathbf{r}' - \mathbf{r}), & i_l = 2m, \\ \delta(\mathbf{k} - \mathbf{k}') \cdot \delta(\mathbf{r}' - \mathbf{r}), & i_l = 2M + 1. \end{cases} \tag{5.11}$$

Combining with the independence assumption in Rule 5, we are able to define a probability measure $\Pi_{Q,t}$ on \mathcal{B}_Ω , the Borel extension of the cylinder sets on Ω [35],

$$\Pi_{Q,t}(\mathbb{1}_E) = \int_{\Omega} \mathbb{1}_E(\omega) \Pi_{Q,t}(d\omega) = \Pr(E), \tag{5.12}$$

as well as a stochastic branching process on the probability space $(\Omega, \mathcal{B}_\Omega, \Pi_{Q,t})$. Since $\omega \in \Omega$ corresponds to a denumerable random sequence, the Kolmogorov extension theorem (see Theorem 6.16 in [41]) ensures the existence and uniqueness of such process.

Moreover, from Eq. (5.10), one can easily verify the Markov property of the stochastic process on the probability space $(\Omega, \mathcal{B}_\Omega, \Pi_{Q,t})$

$$\begin{aligned} \Pi_{Q,t}(XY) &= \Pi_{Q,t}(X\Pi_{Q_i,t+\tau_0}Y) \\ &= \int_{\Omega} X(\omega) \left\{ \int_{\Omega_i} Y(\omega_i) \Pi_{Q_i,t+\tau_0}(d\omega_i) \right\} \Pi_{Q,t}(d\omega) \end{aligned} \quad (5.13)$$

for any measurable function X on the space Ω and Y on $\Omega_i \subset \Omega$. That is, *events observable before and after time $t + \tau_0$ are conditionally independent*.

Next we need to define a signed measure valued function $\mu : (\mathbb{R}^d \times \mathcal{X}, \mathcal{B}) \rightarrow \mathbb{R}$ through the particle weights and the frozen states, where $\mathcal{B} \in \mathcal{B}_\Omega$. According to Rule 4, the frozen state of a particle $\langle i_1 i_2 \cdots i_n \rangle$ is $(\mathbf{r}_{i_1 i_2 \cdots i_n}(T - t_{i_1 i_2 \cdots i_n}), \mathbf{k}_{i_1 i_2 \cdots i_n})$ with $t_{i_1 i_2 \cdots i_n} = t + \tau_0 + \cdots + \tau_{i_1 i_2 \cdots i_{n-1}}$, and the frozen state of $\langle 0 \rangle$ is $(\mathbf{r}_0(T - t), \mathbf{k}_0)$.

Definition 5.4. Suppose $(\mathbf{r}_i, \mathbf{k}_i)$ is the starting state of a frozen particle i in a given family history ω , $w_0 = 1$ is the initial weight and let $\delta_{(\mathbf{r}, \mathbf{k})}$ mean the unit measure concentrated at state (\mathbf{r}, \mathbf{k}) . Then we define the exit measure as follows

$$\mu = \sum_{i \in \mathcal{E}(\omega)} w_i \cdot \delta_{(\mathbf{r}_i(T-t_i), \mathbf{k}_i)}, \quad (5.14)$$

where w_i is the cumulative weight of particle i . For an object $i = \langle i_1 i_2 \cdots i_n \rangle$, w_i is given by

$$w_i = w_0 \cdot \zeta_{i_1}(\mathbf{r}_{i_1}) \cdot \zeta_{i_2}(\mathbf{r}_{i_1 i_2}) \cdots \zeta_{i_{n-1}}(\mathbf{r}_{i_1 i_2 \cdots i_{n-1}}) \cdot \mathbb{1}_{\{\mathbf{k}_{i_1} \in \mathcal{X}, \dots, \mathbf{k}_{i_1 i_2 \cdots i_{n-1}} \in \mathcal{X}\}}, \quad (5.15)$$

and the function $\zeta(\mathbf{r})$ has been defined in Eq. (5.4). Moreover, for given ω and function $A(\mathbf{r}, \mathbf{k})$, we can further define a random integral on the point distribution

$$\mu_A(\omega) = \int A(\mathbf{r}, \mathbf{k}) \mu(d\mathbf{r} \times d\mathbf{k}, \omega) = \sum_{i \in \mathcal{E}(\omega)} w_i \cdot A(\mathbf{r}_i(T - t_i), \mathbf{k}_i). \quad (5.16)$$

To ensure a bounded weight, we require

$$|\zeta_i(\mathbf{r})| \leq 1, \quad \forall \mathbf{r} \in \mathbb{R}^d, \quad \forall i \in \{1, \dots, 2M + 1\}. \quad (5.17)$$

The first moment of random function $\mu_A(\omega)$ is denoted by $\psi(\mathbf{r}, \mathbf{k}, t)$ which reads

$$\psi(\mathbf{r}, \mathbf{k}, t) = \Pi_{Q,t}(\mu_A) = \int_{\Omega} \mu_A(\omega) \Pi_{Q,t}(d\omega). \quad (5.18)$$

Example 5.2. Suppose the ancestor starts at $t = 0$ carrying the initial weight $w = 1$. For the family history ω displayed in Fig. 2, the random integral $\mu_A(\omega)$ is

$$\begin{aligned} \mu_A(\omega) &= \zeta(\mathbf{r}_1)A(\mathbf{r}_1(T - \tau_0), \mathbf{k}_1) + \zeta(\mathbf{r}_2)\zeta(\mathbf{r}_{21})A(\mathbf{r}_{21}(T - \tau_0 - \tau_2), \mathbf{k}_{21}) \\ &\quad + \zeta(\mathbf{r}_2)\zeta(\mathbf{r}_{22})A(\mathbf{r}_{22}(T - \tau_0 - \tau_2), \mathbf{k}_{22}) \\ &\quad + \zeta(\mathbf{r}_2)\zeta(\mathbf{r}_{23})\zeta(\mathbf{r}_{231})A(\mathbf{r}_{231}(T - \tau_0 - \tau_2 - \tau_{23}), \mathbf{k}_{231}) \\ &\quad + \zeta(\mathbf{r}_2)\zeta(\mathbf{r}_{23})\zeta(\mathbf{r}_{232})A(\mathbf{r}_{232}(T - \tau_0 - \tau_2 - \tau_{23}), \mathbf{k}_{232}) \\ &\quad + \zeta(\mathbf{r}_2)\zeta(\mathbf{r}_{23})\zeta(\mathbf{r}_{233})A(\mathbf{r}_{233}(T - \tau_0 - \tau_2 - \tau_{23}), \mathbf{k}_{233}) \\ &\quad + \zeta(\mathbf{r}_3)A(\mathbf{r}_3(T - \tau_0), \mathbf{k}_3). \end{aligned} \quad (5.19)$$

In order to study the particle number in the branching particle system with the family history ω starting from time t , we use a random function $Z(\omega, T - t)$ to stand for the total number of frozen particles at the final instant T . In consequence, the first moment of $Z(\omega, T - t)$ is

$$\mathbb{E}Z_{T-t} = \int_{\Omega} Z(\omega, T - t)\Pi_{Q,t}(d\omega), \quad (5.20)$$

which also gives the expectation of the total number of alive particles in time interval $[t, T]$, and should be finite (see Theorem 5.1). This further means that $Z(\omega, T - t)$ is finite almost surely. As the easier case, the finiteness of $\mathbb{E}Z_{T-t}$ for the constant auxiliary function is directly implied from Theorem 13.1 and its corollary of Chapter VI in [35].

Theorem 5.1 (L^1 -boundedness). *Suppose the family history ω starts at time t at state at state $Q = (\mathbf{r}, \mathbf{k})$, and ends at T . Then $\mathbb{E}Z_{T-t} < \infty$ and as a consequence $\Pr(\{Z(\omega, T - t) < \infty\}) = 1$.*

Proof. We define a random function $\mathbb{1}_{i_1 i_2 \dots i_n}(\omega) = 1$ when the particle $\langle i_1 i_2 \dots i_n \rangle$ appears in the family history ω , otherwise $\mathbb{1}_{i_1 i_2 \dots i_n}(\omega) = 0$. From Eq. (5.12) and Definition 5.3, we have

$$\Pi_{Q,t}(1_{i_1 i_2 \dots i_n}) = \int_{\Omega} \mathbb{1}_{i_1 i_2 \dots i_n}(\omega)\Pi_{Q,t}(d\omega) = \Pr(\{t + \tau_0 + \dots + \tau_{i_1 i_2 \dots i_{n-1}} < T\}). \quad (5.21)$$

Let

$$\bar{Z}(\omega, T - t) = 1 + \sum_{n=1}^{\infty} \sum_{i_1, \dots, i_n=1}^{2M+1} 1_{i_1 i_2 \dots i_n}(\omega), \quad (5.22)$$

that corresponds to the number of particles born up to the final time T . It is obvious that

$$Z(\omega, T - t) \leq \bar{Z}(\omega, T - t). \quad (5.23)$$

For constant γ_0 , we introduce an exponential distribution

$$G(t') = 1 - e^{-\gamma_0(t'-t)}, \quad t' \geq t, \quad (5.24)$$

and define its n -th convolution by

$$G_0(t') = G(t'), \quad G_n(t') = \int_0^{t'} G_{n-1}(t' - u) dG(u). \quad (5.25)$$

It can be readily verified that

$$\frac{d\mathcal{G}(t'; \mathbf{r}, u)}{dt'} \leq \frac{k}{2M+1} \cdot \frac{dG(t')}{dt'}, \quad \forall t' \in [u, T], \quad \forall \mathbf{r} \in \mathbb{R}^d, \quad \forall u \in [0, T] \quad (5.26)$$

holds for a sufficiently large integer k , e.g., $k > (2M+1)e^{\gamma_0 T}$.

We first show by the mathematical induction that there exists a sufficient large integer k and a sufficient large constant $\gamma_0 > 0$ such that

$$\begin{aligned} & \Pr\left(\{t + \tau_0 + \dots + \tau_{i_1 i_2 \dots i_{n-1}} < T - u\}\right) \\ & \leq \left(\frac{k}{2M+1}\right)^{n-1} G_{n-1}(T - u), \quad \forall u \in [0, T - t]. \end{aligned} \quad (5.27)$$

For $n = 1$, we only need $\gamma_0 \geq \max\{\gamma(\mathbf{r})\}$ and then have

$$\begin{aligned} \Pr(\{t + \tau_0 < T - u\}) &= \frac{d\mathcal{G}(t'; \mathbf{r}, t)}{dt'} \Big|_{t'=T-u} \\ &= 1 - e^{-\int_t^{T-u} \gamma(\mathbf{r}(s-t)) ds} \leq 1 - e^{-\gamma_0(T-u-t)} = G_0(T - u). \end{aligned} \quad (5.28)$$

Assume Eq. (5.27) is true for n . Direct calculation shows

$$\begin{aligned} & \Pr\left(\{t + \tau_0 + \dots + \tau_{i_1 i_2 \dots i_n} < T - u\}\right) = \Pi_{Q,t}\left(\mathbb{1}_{\{t + \tau_0 + \dots + \tau_{i_1 i_2 \dots i_n} < T - u\}}\right) \\ &= \int_0^{T-t-u} \Pi_{Q,t}\left(\mathbb{1}_{\{t + \tau_0 + \dots + \tau_{i_1 i_2 \dots i_{n-1}} < T - u - v\}} \mathbb{1}_{\{\tau_{i_1 i_2 \dots i_n} < v\}}\right) dv \\ &= \int_0^{T-t-u} \Pi_{Q,t}\left(\mathbb{1}_{\{t + \tau_0 + \dots + \tau_{i_1 i_2 \dots i_{n-1}} < T - u - v\}} \cdot \Pi_{Q_{i_1 \dots i_n, t_{i_1} \dots i_n}}(\mathbb{1}_{\{\tau_{i_1 i_2 \dots i_n} < v\}})\right) dv \\ &\leq \int_0^{T-t-u} \left(\frac{k}{2M+1}\right)^{n-1} G_{n-1}(T - u - v) \cdot \frac{k}{2M+1} dG(v) \\ &= \left(\frac{k}{2M+1}\right)^n G_n(T - u), \end{aligned} \quad (5.29)$$

which implies that Eq. (5.27) holds for $n + 1$.

Finally, using Eqs. (5.21) and (5.27) yields

$$\begin{aligned} & \int_{\Omega} \bar{Z}(\omega, T - t) \Pi_{Q,t}(d\omega) \\ &= 1 + \sum_{n=1}^{\infty} \sum_{i_1, \dots, i_n=1}^{2M+1} \Pi_{Q,t}(\mathbb{1}_{i_1 i_2 \dots i_n}) \leq 1 + (2M+1) \sum_{n=1}^{\infty} k^{n-1} G_{n-1}(T), \end{aligned} \quad (5.30)$$

and implies $\int_{\Omega} \bar{Z}(\omega, T-t) \Pi_{Q,t}(d\omega)$ is bounded for the infinite series is convergent (see Lemma 1 of the Appendix to Chapter VI in [35]). Hence the proof is completed according to Eq. (5.23).

Moreover, according to Definition 5.4 and Theorem 5.1, we can directly show that μ_A is integrable, say,

$$\int_{\Omega} |\mu_A(\omega)| \Pi_{Q,t}(d\omega) < \infty \quad (5.31)$$

provided that $A(\mathbf{r}, \mathbf{k})$ is essentially bounded. That is, both μ_A in Eq. (5.16) and ψ in Eq. (5.18) are well defined.

With the above preparations, we begin to present the main theorem.

Theorem 5.2 (Stochastic interpretation of the strong solution). *The first moment $\psi(\mathbf{r}, \mathbf{k}, t)$ defined in Eq. (5.18) equals to the solution of the adjoint equation (4.38).*

Proof. Let $E = \{\tau_0 : t + \tau_0 \geq T\} \cap \Omega$ correspond to the case in which the particle travels to $(\mathbf{r}(T-t), \mathbf{k})$ and then is frozen. The probability of such event is $1 - \mathcal{G}(T; \mathbf{r}, t)$ by Rule 4. Then the remaining case is denoted by $E^c = \{\tau_0 : t + \tau_0 < T\} \cap \Omega$. Accordingly, from Eq. (5.18), we have

$$\psi(\mathbf{r}, \mathbf{k}, t) = \int_E \mu_A(\omega) \Pi_{Q,t}(d\omega) + \int_{E^c} \mu_A(\omega) \Pi_{Q,t}(d\omega), \quad (5.32)$$

and a direct calculation gives

$$\int_E \mu_A(\omega) \Pi_{Q,t}(d\omega) = \mathbb{E}^{-\int_t^T \gamma(\mathbf{r}(s-t)) ds} A(\mathbf{r}(T-t), \mathbf{k}), \quad (5.33)$$

which recovers the first right-hand-side term of Eq. (4.38). When event E^c occurs, it indicates that $2M+1$ offsprings are generated. Notice that $\omega = (Q_0; \omega_1; \omega_2; \dots; \omega_{2M+1})$ and thus we have

$$\mu_A(\omega) = \sum_{i=1}^{2M+1} w_i \cdot \mu_A(\omega_i) = \sum_{i=1}^{2M+1} \zeta_i(\mathbf{r}(\tau_0)) \cdot \mathbb{1}_{\mathcal{X}}(\mathbf{k}_i) \cdot \mu_A(\omega_i), \quad (5.34)$$

where we have applied Rule 3.

Substitute Eq. (5.34) into the second right-hand-side term of Eq. (5.32) leads to

$$\begin{aligned} & \int_{E^c} \mu_A(\omega) \Pi_{Q,t}(d\omega) \\ &= \sum_{i=1}^{2M+1} \int_{E^c \cap \{\mathbf{k}_i \in \mathcal{X}\}} \zeta_i(\mathbf{r}(\tau_0)) \left\{ \int_{\Omega_i} \mu_A(\omega_i) \Pi_{Q_i, t+\tau_0}(d\omega_i) \right\} \Pi_{Q,t}(d\omega), \end{aligned} \quad (5.35)$$

where we have used the Markov property (5.13) as well as the mutual independence among the subfamilies inherited in Rule 5.

Finally, by the definition (5.18), we have

$$\int_{\Omega_i} \mu_A(\omega_i) \Pi_{Q_i, t+\tau_0}(d\omega_i) = \psi(\mathbf{r}_i, \mathbf{k}_i, t + \tau_0), \quad i = 1, \dots, 2M + 1. \quad (5.36)$$

Then the first right-hand-side term of Eq. (5.35) becomes

$$\begin{aligned} & \int_{E^c \cap \{\mathbf{k}_1 \in \mathcal{X}\}} \zeta_1(\mathbf{r}(\tau_0)) \psi(\mathbf{r}_1, \mathbf{k}_1, t + \tau_0) \Pi_{Q, t}(d\omega) \\ &= \int_t^T dt_1 e^{-\int_t^{t_1} \gamma(\mathbf{r}(s-t)) ds} \int_{\mathcal{X}} d\mathbf{k}_1 \{V_w^-(\mathbf{r}(t_1 - t), \mathbf{k} - \mathbf{k}_1)\} \psi(\mathbf{r}_1, \mathbf{k}_1, t_1), \end{aligned} \quad (5.37)$$

where we have let $t + \tau_0 \rightarrow t_1$ and used Eqs. (5.4) and (5.11). The remaining right-hand-side term of Eq. (5.35) terms can be treated in a similar way, and putting them together recovers the second right-hand-side term of Eq. (4.38). The proof is completed. \square

So far we have proven the existence of the solution of the adjoint equation (4.38), while its uniqueness can be deduced by the Fredholm alternative.

Our next goal is to show that the probabilistic interpretation of the weak solution of the Wigner equation is readily established by an extension of the probability space $(\Omega, \mathcal{B}_\Omega, \Pi_{Q, t})$. Intuitively speaking, it is motivated by the randomization of the initial state Q . To overcome the problem induced by the negative values of $f(\mathbf{r}, \mathbf{k}, 0)$, we define an instrumental probability density function f_I as

$$f_I(\mathbf{r}, \mathbf{k}) = \frac{|f(\mathbf{r}, \mathbf{k}, 0)|}{\iint_{\mathbb{R}^d \times \mathbb{R}^d} |f(\mathbf{r}, \mathbf{k}, 0)| d\mathbf{r} d\mathbf{k}}, \quad (5.38)$$

which gives a probability measure λ_I on $\mathbb{R}^d \times \mathbb{R}^d$ as $d\lambda_I = f_I(\mathbf{r}, \mathbf{k}) d\mathbf{r} d\mathbf{k}$.

Definition 5.5. *The extension $(\hat{\Omega}, \hat{\mathcal{B}}_\Omega, \hat{\Pi}_t)$ of the probability space $(\Omega, \mathcal{B}_\Omega, \Pi_{Q, t})$ is*

$$\hat{\Omega} = \mathbb{R}^d \times \mathbb{R}^d \times \Omega, \quad \hat{\mathcal{B}}_\Omega = \mathcal{R}^d \otimes \mathcal{R}^d \otimes \mathcal{B}_\Omega, \quad \hat{\Pi}_t = \lambda_I \otimes \Pi_{Q, t}. \quad (5.39)$$

For any measurable function X on Ω , the extended probability measure $\hat{\Pi}_t$ reads

$$\hat{\Pi}_t X = \lambda_I \otimes \Pi_{Q, t}(X) = \iint_{\mathbb{R}^{2d}} f_I(\mathbf{r}, \mathbf{k}) \left\{ \int_{\Omega} X(\omega) \Pi_{Q, t}(d\omega) \right\} d\mathbf{r} d\mathbf{k}. \quad (5.40)$$

The following theorem characterizes the probabilistic interpretation of the inner product $\langle \hat{A} \rangle_T$ and serves as the mathematical foundation of wpWBRW. Its numerical counterpart will be discussed in Section 5.3.

Theorem 5.3 (Stochastic interpretation of the weak solution). *Suppose $A(\mathbf{r}, \mathbf{k})$ has a compact support in \mathcal{X} and define*

$$s(\mathbf{r}, \mathbf{k}) = f(\mathbf{r}, \mathbf{k}, 0) / f_I(\mathbf{r}, \mathbf{k}), \quad (5.41)$$

then the inner product $\langle \hat{A} \rangle_T$ is represented as

$$\langle \hat{A} \rangle_T = \lambda_I \otimes \Pi_{Q,0}(s \cdot \mu_A) = \iint_{\mathbb{R}^{2d}} s(\mathbf{r}, \mathbf{k}) \left\{ \int_{\Omega} \mu_A(\omega) \Pi_{Q,0} d\omega \right\} d\mathbf{r} d\mathbf{k}. \quad (5.42)$$

Proof. Combining Eq. (4.31) and Theorem 5.2, it is readily verified that

$$\begin{aligned} \lambda_I \otimes \Pi_{Q,0}(s \cdot \mu_A) &= \iint_{\mathbb{R}^{2d}} f_I(\mathbf{r}, \mathbf{k}) \left\{ s(\mathbf{r}, \mathbf{k}) \int_{\Omega} \mu_A(\omega) \Pi_{Q,0}(d\omega) \right\} d\mathbf{r} d\mathbf{k} \\ &= \iint_{\mathbb{R}^{2d}} f_I(\mathbf{r}, \mathbf{k}) \left\{ \frac{f(\mathbf{r}, \mathbf{k}, 0)}{f_I(\mathbf{r}, \mathbf{k})} \int_{\Omega} \mu_A(\omega) \Pi_{Q,0}(d\omega) \right\} d\mathbf{r} d\mathbf{k} \\ &= \iint_{\mathbb{R}^{2d}} f(\mathbf{r}, \mathbf{k}, 0) \varphi(\mathbf{r}, \mathbf{k}, 0) d\mathbf{r} d\mathbf{k} = \langle \hat{A} \rangle_T. \end{aligned} \quad (5.43)$$

The proof is finished. \square

5.3. Importance sampling and the particle sign

Hereto we have shown the connection between the average $\langle \hat{A} \rangle_T$ and a stochastic process in Theorem 5.3. Naturally, $\langle \hat{A} \rangle_T$ can be evaluated through the sequential importance sampling [44]. By exploiting the Markovian property of the linear evolution system, it suffices to divide the total time $[0, t_{fin}]$ into n steps, denoted by $0 = t_0 \leq t_1 \leq t_2 \cdots \leq t_{n-1} \leq t_n = t_{fin}$ and we investigate the time interval $[t_l, t_{l+1}]$ and set $f(\mathbf{r}, \mathbf{k}, t_l)$ as the initial condition, without loss of generality.

Regarding of the fact that the Wigner function may take negative value, we have to introduce an *instrumental probability distribution* f_I as in Eq. (5.38)

$$f_I(\mathbf{r}, \mathbf{k}, t) = \frac{1}{H(t)} \left| f(\mathbf{r}, \mathbf{k}, t) \right|, \quad (5.44)$$

where $H(t)$ is the normalizing factor (we assume $f \in L^1(\mathbb{R}^d \times \mathcal{X})$)

$$H(t) = \iint_{\mathbb{R}^d \times \mathcal{X}} \left| f(\mathbf{r}, \mathbf{k}, t) \right| d\mathbf{r} d\mathbf{k}. \quad (5.45)$$

Now the inner product problem can be evaluated by the following estimator

$$\langle A \rangle_{t_{l+1}} \approx \frac{\sum_{\alpha} s_{\alpha}(t_l) \cdot \Pi_{Q_{\alpha}, t_l}(\mu_A)}{\sum_{\alpha} s_{\alpha}(t_l)} = \frac{\sum_{\alpha} s_{\alpha}(t_l) \cdot \Pi_{Q_{\alpha}, t_l}(\mu_A)}{\sum_{\alpha} s_{\alpha}(t_l)}, \quad (5.46)$$

where $Q_{\alpha} = (\mathbf{r}_{\alpha}, \mathbf{k}_{\alpha})$ are draws from f_I and the particle sign function s_{α} reads

$$s_{\alpha}(t) = \frac{f(\mathbf{r}_{\alpha}, \mathbf{k}_{\alpha}, t)}{f_I(\mathbf{r}_{\alpha}, \mathbf{k}_{\alpha}, t) H(t)} \quad (5.47)$$

being either -1 or 1 due to Eq. (5.44). Here $s_\alpha(t)$ can be regarded as the numerical counterpart of Eq. (5.41). In fact, the estimator adopted in Eq. (5.46) implicitly utilizes the strong law of large number

$$\frac{1}{N_\alpha} \sum_\alpha H(t) s_\alpha(t) \rightarrow 1 \text{ as } N_\alpha \rightarrow +\infty, \text{ a.s.}, \quad (5.48)$$

Furthermore, according to Theorem 5.2, $\Pi_{Q_\alpha, t_l}(\mu_A)$ can be estimated by

$$\Pi_{Q_\alpha, t_l}(\mu_A) \approx \sum_{i \in \mathcal{E}(\omega_\alpha)} w_{i, \alpha}(t_l) \cdot A(\mathbf{r}_{i, \alpha}, \mathbf{k}_{i, \alpha}), \quad (5.49)$$

where $\{\mathbf{r}_{i, \alpha}, \mathbf{k}_{i, \alpha}\}$ are frozen particles starting from the ancestor $(\mathbf{r}_\alpha, \mathbf{k}_\alpha)$. Then substituting Eq. (5.49) into Eq. (5.46) yields

$$\langle A \rangle_{t_{l+1}} \approx \left\langle A, \frac{1}{N_\alpha} \sum_\alpha \sum_{i \in \mathcal{E}_\alpha} s_\alpha(t_l) \cdot w_{i, \alpha}(t_l) \cdot \delta_{(\mathbf{r}_{i, \alpha}, \mathbf{k}_{i, \alpha})} \right\rangle_0, \quad (5.50)$$

where the inner product $\langle \cdot, \cdot \rangle_0$ is the same as in Eq. (4.39) and $N_\alpha = \sum_\alpha s_\alpha$ is the sample size, that is a conserved quantity. In this manner, $\langle \hat{A} \rangle$ is evaluated by a purely particle-based scheme in which every super-particle, carrying a weight and a sign, is moving according to several specific rules in the branching particle system.

Notice that the sample size N_α is the numerical counterpart of the total mass in Eq. (3.2), instead of the particle number. The following theorem presents that N_α is a conserved quantity after branching, so does the total mass.

Theorem 5.4 (Mass conservation). *Suppose that the ancestor particle starts at $t = 0$ and carries a weight $w_0 = 1$ and two particles carrying the same weight but opposite sign are generated in pair, then we have*

$$\Pr(\mathbf{E}) = \int_\Omega \mathbb{1}_{\mathbf{E}}(\omega) \Pi_{Q, 0}(d\omega) = 1, \quad (5.51)$$

where the event \mathbf{E} is given by

$$\mathbf{E} = \left\{ \omega \in \Omega : \sum_{i \in \mathcal{E}(\omega)} w_i = 1 \right\}. \quad (5.52)$$

Proof. Since $Z(\omega, T - t)$ only takes odd values, it suffices to take

$$\mathbf{E}_n = \left\{ \omega \in \Omega : \sum_{i \in \mathcal{E}(\omega)} w_i = 1; Z(\omega, T - t) \leq 2n + 1 \right\}, \quad (5.53a)$$

$$\mathbf{E}_n^* = \left\{ \omega \in \Omega : Z(\omega, T - t) \leq 2n + 1 \right\}, \quad (5.53b)$$

and it is easy to see $\Pr(\mathbf{E}_0) = \Pr(\mathbf{E}_0^*)$. In the remaining part of the proof, we will omit $\omega \in \Omega$ for brevity. Assume that the statement that $\Pr(\mathbf{E}_k) = \Pr(\mathbf{E}_k^*)$ is true for $0 \leq k \leq n$, $\forall t \in [0, T]$. We show below by the mathematical induction that it still holds for $k = n + 1$.

From $\omega = (Q_0; \omega_1; \dots; \omega_{2M+1})$, it can be easily verified that

$$Z(\omega, T - t) = \sum_{l=1}^{2M+1} Z(\omega_l, T - t - \tau_0), \quad (5.54)$$

thus we have

$$Z(\omega_l, T - t - \tau_0) < Z(\omega, T - t), \quad \forall l \in \{1, 2, \dots, 2M+1\} \quad (5.55)$$

implying

$$E_{n+1}^* \subset \{Z(\omega_l, T - t - \tau_0) \leq 2n + 1\}, \quad \forall l \in \{1, 2, \dots, 2M+1\}. \quad (5.56)$$

Furthermore, since $\zeta_{2m-1}(\mathbf{r}) = -\zeta_{2m}(\mathbf{r})$, it yields

$$\sum_{i \in \mathcal{E}(\omega)} w_i = \sum_{m=1}^M \zeta_{2m-1}(\mathbf{r}(\tau_0)) \cdot \left\{ \sum_{i \in \mathcal{E}(\omega_{2m-1})} w_i - \sum_{i \in \mathcal{E}(\omega_{2m})} w_i \right\} + \sum_{i \in \mathcal{E}(\omega_{2M+1})} w_i, \quad (5.57)$$

we obtain

$$\bigcap_{l=1}^{2M+1} \left\{ \sum_{i \in \mathcal{E}(\omega_l)} w_i = 1 \right\} \subset \left\{ \sum_{i \in \mathcal{E}(\omega)} w_i = 1 \right\}. \quad (5.58)$$

Combining Eqs. (5.56) and (5.58) with the conditionally independence of ω_l yields

$$\begin{aligned} \frac{\Pr(E_{n+1})}{\Pr(E_{n+1}^*)} &\geq \Pr \left(\bigcap_{l=1}^{2M+1} \left\{ \sum_{i \in \mathcal{E}(\omega_l)} w_i = 1 \right\} \middle| E_{n+1}^* \right) = \prod_{l=1}^{2M+1} \Pr \left(\left\{ \sum_{i \in \mathcal{E}(\omega_l)} w_i = 1 \right\} \middle| E_{n+1}^* \right) \\ &= \prod_{l=1}^{2M+1} \Pr(\{ \sum_{i \in \mathcal{E}(\omega_l)} w_i = 1, Z(\omega, T - t) \leq 2n + 3 \}) / \Pr(E_{n+1}^*) = 1, \end{aligned}$$

where the induction hypothesis is applied in the last line, and thus $\Pr(E_{n+1}) \geq \Pr(E_{n+1}^*)$. Accordingly, we have $\Pr(E_{n+1}) = \Pr(E_{n+1}^*)$ for it is obvious that $\Pr(E_{n+1}) \leq \Pr(E_{n+1}^*)$.

Finally, according to the fact that $E_0 \subset E_1 \subset \dots \subset E_n \subset E_{n+1} \subset \dots \subset E$, we have

$$\Pr(E) = \lim_{n \rightarrow +\infty} \Pr(E_n) = 1, \quad (5.59)$$

due to the monotone convergence theorem. Hence we complete the proof by setting $t = 0$.

By taking $A = \mathbb{1}_{\mathbb{R}^d \times \mathcal{K}}$, one is readily to verify that

$$\int_{\mathbb{R}^d} d\mathbf{r} \int_{\mathcal{K}} d\mathbf{k} f(\mathbf{r}, \mathbf{k}, T) \approx \frac{1}{N_\alpha} \sum_{\alpha} \sum_{i \in \mathcal{E}_\alpha} s_\alpha(t_l) \cdot w_{i,\alpha}(t_l) = \frac{1}{N_\alpha} \sum_{\alpha} s_\alpha(t_l) = 1, \quad (5.60)$$

and then it further implies

$$\int_{\mathbb{R}^d} d\mathbf{r} \int_{\mathcal{K}} d\mathbf{k} f(\mathbf{r}, \mathbf{k}, T) = \int_{\mathbb{R}^d} d\mathbf{r} \int_{\mathcal{K}} d\mathbf{k} f(\mathbf{r}, \mathbf{k}, 0), \quad \forall T \geq 0, \quad (5.61)$$

due to Eqs. (4.20) and (4.31), which is nothing but the mass conservation (3.3).

5.4. Resampling

Apart from the probabilistic interpretation and the importance sampling, the resampling is another major component for a computable wpWBRW. Before discussing the basic idea of resampling, we first need to clarify its necessity.

It starts by estimating the growth rate of particles in the branching system. For the constant auxiliary function $\gamma(\mathbf{r}) \equiv \gamma_0$, the random life-length τ of a particle starting at time t is characterized by an exponential distribution

$$G(t') = \Pr(\tau < t' - t) = 1 - e^{-\gamma_0(t'-t)}, \quad t' \geq t. \quad (5.62)$$

In this case, the growth of particle number has been thoroughly studied in the literature [35, 45] and we are able to obtain a simple calculation formula of the particle number as shown in Theorem 5.5.

Theorem 5.5 (Exponential growth of particle number). *Suppose the family history ω starts at $t = 0$ and the constant auxiliary function $\gamma(\mathbf{r}) \equiv \gamma_0$ is adopted. Then the expectation of the total number of frozen particles in time interval $[0, T]$ is*

$$\mathbb{E}Z_T = e^{2M\gamma_0 T}. \quad (5.63)$$

Proof. According to Theorem 15.1 of Chapter VI in [35], the expectation $\mathbb{E}Z_{t'}$ satisfies the following renewal integral equation

$$\mathbb{E}Z_{t'} = 1 - G(t') + (2M + 1) \int_0^{t'} \mathbb{E}Z_{t'-u} dG(u), \quad \mathbb{E}Z_0 = 1. \quad (5.64)$$

We substitute Eq. (5.62) into Eq. (5.64) and then can easily verify that $\mathbb{E}Z_{t'} = e^{2M\gamma_0 t'}$ is the solution. The proof is finished. \square

Considering the fact that randomly generated \mathbf{k}' may be rejected in numerical application according to the indicator function in Eq. (5.15), we can modify Eq. (5.64) by replacing $2M + 1$ with $2\alpha_0 M + 1$, with α_0 the average acceptance ratio of \mathbf{k}' . In consequence, the modified expectation of total particle number is $\mathbb{E}Z_T = e^{2\alpha_0 M \gamma_0 T}$.

Theorem 5.5 also provides an upper bound of $\mathbb{E}Z_T$ when the variable auxiliary function satisfies $\gamma(\mathbf{r}) \leq \gamma_0$. Whatever the auxiliary function is, it is clear that the particle number will grow exponentially. *In order to suppress the particle number, we can either decrease the parameter γ_0 or choose a smaller final time T .*

Finally, suppose we would like to evolve the branching particle system until the final time T and there are two typical ways. One is to evolve the system until each particle is frozen at the final time T in a single step. The other is to divide T into $0 = t_0 < t_1 < \dots < t_{n-1} < t_n = T$ with $t_n = n\Delta t$ and Δt being the time step, and then we evolve the system successively in n steps. The latter is usually adopted to measure quantum observables at instants t_n . However, the following theorem tells us that both ways produce the same $\mathbb{E}Z_T$.

Theorem 5.6 (Markovian character of the particle number, Theorem 11.1 of Chapter VI in [35]). *Suppose $G(t) = 1 - e^{-\gamma_0 t}$. Then $Z(\omega, t)$ is a Markov branching process. In addition, $Z(\omega, \Delta t), Z(\omega, 2\Delta t), \dots$ is a Galton-Watson process.*

We recall that for a Galton-Watson model, if $\mathbb{E}Z_{\Delta t} = \beta$, then $\mathbb{E}Z_{n\Delta t} = \beta^n$. From Eq. (5.63), we know that $\beta = e^{2M\gamma_0\Delta t}$, so that $\mathbb{E}Z_{n\Delta t} = e^{2M\gamma_0 T}$. Therefore, we cannot expect to reduce the particle number by simply dividing T into several steps and evolve the particle system successively, which also manifests the indispensability of resampling.

Theorem 5.5 has uncovered an embarrassing situation that the particle number in the branching particle system will grow exponentially in time, which have also been observed in numerical simulations [46]. The naive splitting of time, say, dividing T into n intervals, fails to save the efficiency according to Theorem 5.6. In this regard, the particle resampling is performed every few steps to both reduce the particle number and suppress the stochastic errors [46–48]. Mathematically speaking, the resampling is consisted of two procedures: the reconstruction of the Wigner function from the weighted empirical measure (density estimation) and the generation of new particles from the reconstructed Wigner function (sampling).

The reconstruction, formulated by Eq. (5.65), is also termed the density estimation in statistical terminology.

$$\left\langle A, \frac{1}{N_0} \sum_{\alpha} \sum_{i \in \mathcal{E}_{\alpha}} s_i(t_l) \cdot w_{i,\alpha}(t_l) \cdot \delta_{(r_{i,\alpha}, \mathbf{k}_{i,\alpha})} \right\rangle_0 \approx \langle A, p(t_{l+1}) \rangle_0. \quad (5.65)$$

The pivotal issue in the density estimation is to choose an appropriate form of $p(\mathbf{r}, \mathbf{k}, t_{l+1})$. In general, one can pick up two basis $\{\phi_{\mu}(\mathbf{r}), \mu \in \mathbb{Z}^n\}$ and $\{\psi_{\nu}(\mathbf{k}), \nu \in \mathbb{Z}^n\}$ in \mathbf{x} -space and \mathbf{k} -space, respectively, and set

$$p(\mathbf{r}, \mathbf{k}, t_{l+1}) = \sum_{\mu \in \mathbb{Z}^n} \sum_{\nu \in \mathbb{Z}^n} \beta_{\mu,\nu}(t_{l+1}) \phi_{\mu}(\mathbf{r}) \psi_{\nu}(\mathbf{k}). \quad (5.66)$$

The basis can be either orthogonal or not orthogonal, such as the piecewise constant function, the Fourier basis [48] and the Gaussian wave packets [43]. Here we only concern the most ubiquitous choice: the piecewise constant function

$$\phi_{\mu}(\mathbf{r}) \psi_{\nu}(\mathbf{k}) = |D_{\mu,\nu}|^{-1} \cdot \mathbb{1}_{D_{\mu,\nu}}(\mathbf{r}, \mathbf{k}), \quad (5.67)$$

where the domain $\mathbb{R}^d \times \mathcal{K} = \bigcup_{\mu,\nu} D_{\mu,\nu}$ and $D_{\mu,\nu}$ are mutually disjoint. One can readily verify the orthogonality.

$$\langle \phi_{\mu} \psi_{\nu}, \phi_{\tilde{\mu}} \psi_{\tilde{\nu}} \rangle_0 = \begin{cases} 1, & \mu = \tilde{\mu}, \nu = \tilde{\nu}, \\ 0, & \text{otherwise.} \end{cases} \quad (5.68)$$

Such an approximation borrows the idea of the *histogram statistics*. In other fields, it is also termed the particle cancelation or annihilation as the particles in the same cell with opposite signs will be cancelled out. This choice is the simplest, but perhaps the most

attractive. It has been widely used in the Direct simulation of Monte Carlo method for the Boltzmann equation [47] and the signed-particle Wigner Monte Carlo method [28,29,31].

The coefficients $\beta_{\mu,\nu}(t_{l+1})$ are estimated by the Wigner probability on the domain $D_{\mu,\nu}$

$$\beta_{\mu,\nu}(t_{l+1}) = W_{D_{\mu,\nu}}(t_{l+1}) \approx \frac{1}{N_0} \frac{1}{|D_{\mu,\nu}|} \sum_{\alpha} \sum_{i \in \mathcal{E}_{\alpha}(\omega)} s_i(t_l) \cdot w_{i,\alpha}(t_l) \cdot \mathbb{1}_{D_{\mu,\nu}}(\mathbf{r}_{i,\alpha}, \mathbf{k}_{i,\alpha}). \quad (5.69)$$

Once $p(\mathbf{r}, \mathbf{k}, t_l)$ is obtained, it can be used as the initial state for the next step, with the corresponding instrumental distribution function taking the form as

$$f_I(\mathbf{r}, \mathbf{k}, t_{l+1}) = \frac{1}{H(t_{l+1})} \sum_{\mu \in \mathbb{Z}^n} \sum_{\nu \in \mathbb{Z}^n} |\beta_{\mu,\nu}(t_{l+1})| \phi_{\mu}(\mathbf{r}) \psi_{\nu}(\mathbf{k}). \quad (5.70)$$

For more details, one can refer to [46].

When a uniform partition is adopted, the approach is quite attractive for $d = 1$ and $d = 2$ as it can reduce the particle number effectively, whereas its efficiency deteriorates apparently as the dimension d increases. The possible reason is that dimension of the feature space (the number of bins), that grows exponentially in d , becomes too much higher than the sample size, leading to a non-sparse structure and severe over-fitting [34, 43, 49]. A promising way to resolve this problem is the adaptive partitioning of phase space.

Resampling in a higher dimensional space is a complicated issue and beyond the scope of this paper, and thus left for our future work. In Section 6, we focus on several typical tests for $d = 1, 2$ and show the accuracy of wpWBRW and the histogram statistics by comparing with two deterministic solvers: SEM [23] and ASM [24].

5.5. Outline of wpWBRW

In summary, the outline of wpWBRW is illustrated below from t_l to t_{l+1} with the time step Δt , $l = 1, 2, \dots, n-1$. It suffices to take $\mathbf{r} = \mathbf{r}_{\alpha}, \mathbf{k} = \mathbf{k}_{\alpha}, t = t_l$ as the initial state, and $\mathbf{r}' = \mathbf{r}'_{\alpha}, \mathbf{k}' = \mathbf{k}'_{\alpha}, t' = t'_{\alpha}$ for the offsprings in Eq. (4.43).

Step 1: Sample from $f_I(\mathbf{r}, \mathbf{k}, t_l)$ The first step is to sample N_{α} ancestor particles according to the instrumental distribution $f_I(\mathbf{r}, \mathbf{k}, t_l)$ (see Eq. (5.44)). Each particle has a state $(\mathbf{r}_{\alpha}, \mathbf{k}_{\alpha})$ and carries an initial weight $w_{0,\alpha} = 1$ and a sign s_{α} .

Step 2: Evolve the particles The second step is to evolve super-particles according to the rules of branching particle systems. Suppose a particle is born at $t'_{\alpha} \in [t_l, t_{l+1}]$ at state $(\mathbf{r}'_{\alpha}, \mathbf{k}'_{\alpha})$ with weight w_{α} , and it has a random life-length τ'_{α} satisfying

$$\tau'_{\alpha} \propto \left. \frac{d\mathcal{G}(t'; \mathbf{r}'_{\alpha}, t'_{\alpha})}{dt'} \right|_{t'=t'_{\alpha}+\tau'_{\alpha}} = \gamma(\mathbf{r}'_{\alpha}(\tau'_{\alpha})) e^{-\int_{t'_{\alpha}}^{t'_{\alpha}+\tau'_{\alpha}} \gamma(\mathbf{r}'_{\alpha}(s-t'_{\alpha})) ds}. \quad (5.71)$$

For the ancestor particle, we have $t'_{\alpha} = t_l$, $(\mathbf{r}'_{\alpha}, \mathbf{k}'_{\alpha}) = (\mathbf{r}_{\alpha}, \mathbf{k}_{\alpha})$, $w'_{\alpha} = w_{\alpha}$.

If $\tau'_\alpha \geq t_{l+1} - t'_\alpha$, the particle is frozen at the state $(\mathbf{r}'_\alpha(t_{l+1} - t'_\alpha), \mathbf{k}'_\alpha)$ and the probability of this event is

$$\Pr(\tau'_\alpha \geq t_{l+1} - t'_\alpha) = 1 - \mathcal{G}(t_{l+1}; \mathbf{r}'_\alpha, t'_\alpha) = \mathbb{e}^{-\int_{t'_\alpha}^{t_{l+1}} \gamma(\mathbf{r}'_\alpha(s-t'_\alpha)) ds}. \quad (5.72)$$

Otherwise, the particle travels to a new position $\mathbf{r}'_\alpha(\tau'_\alpha)$ and dies at time $t'_\alpha + \tau'_\alpha$ at state $(\mathbf{r}'_\alpha(\tau'_\alpha), \mathbf{k}'_\alpha)$, and meanwhile, several new particles are generated according to Rule 3, the probability of which is $\mathcal{G}(t'_\alpha + \tau'_\alpha; \mathbf{r}'_\alpha, t'_\alpha)$.

Step 3: Resampling Once all particles in the branching system are frozen, one can record their positions, wavevectors, and weights. Let \mathcal{E}_α denote the index set of all frozen particles with the same ancestor initially at state $(\mathbf{r}_\alpha, \mathbf{k}_\alpha)$, $\{(\mathbf{r}_{i,\alpha}, \mathbf{k}_{i,\alpha}), i \in \mathcal{E}_\alpha\}$ the collection of corresponding frozen states, and $w_{i,\alpha}$ the updated weight of the i -th particle. Accordingly, $\langle \hat{A} \rangle_{t_{l+1}}$ can be estimated as

$$\langle \hat{A} \rangle_{t_{l+1}} \approx \sum_\alpha \sum_{i \in \mathcal{E}_\alpha} s_\alpha(t_l) \cdot w_{i,\alpha}(t_l) \cdot A(\mathbf{r}_{i,\alpha}, \mathbf{k}_{i,\alpha}). \quad (5.73)$$

Particularly, plugging into $A(\mathbf{r}, \mathbf{k}) = \mathbb{1}_D(\mathbf{r}, \mathbf{k})$, we obtain $W_D(\mathbf{r}, \mathbf{k})$. Based on a good partition of phase space: $\mathbb{R}^d \times \mathcal{K} = \bigcup_{\mu, \nu} D_{\mu, \nu}$, we are able to update the instrumental density function $f_I(\mathbf{r}, \mathbf{k}, t_{l+1})$ by the histogram (5.66).

6. Numerical experiments

In order to investigate the performance of the wpWBRW algorithm as well as to verify the theoretical predictions as we discussed earlier such as the effect of constant γ_0 , the increasing behavior of the particle number and the effect of the time step and the annihilation frequency, we simulate a one-body Gaussian barrier scattering in 2D phase space and a two-body Helium-like system in 4D phase space. The relative L^2 error is adopted to study the accuracy. Here $f^{\text{ref}}(x, k, t)$ denotes the reference Wigner function (wf), which could be the exact solution or the numerical solution produced by ASM or SEM on a fine grid mesh, and $f^{\text{num}}(x, k, t)$ is the numerical solution produced by wpWBRW. Then, the relative errors are written as

$$\text{err}_{wf}(t) = \sqrt{\frac{\int_{\mathcal{X} \times \mathcal{K}} (\Delta f(x, k, t))^2 dx dk}{\int_{\mathcal{X} \times \mathcal{K}} (f^{\text{ref}}(x, k, t))^2 dx dk}}, \quad (6.1)$$

where $\Delta f(x, k, t) = |f^{\text{num}}(x, k, t) - f^{\text{ref}}(x, k, t)|$, and the integrals above are evaluated using a simple rectangular rule over a uniform mesh. Under the same sample size N_α , the relative L^2 error in fact measures both the variance of the stochastic algorithm and the errors induced by resampling. To obtain a more complete view of the accuracy, we also measure corresponding relative errors for physical quantities, e.g., the spatial marginal (sm) probability distribution and the momental marginal (mm) probability distribution in a similar way, denoted by $\text{err}_{sm}(t)$ and $\text{err}_{mm}(t)$, respectively.

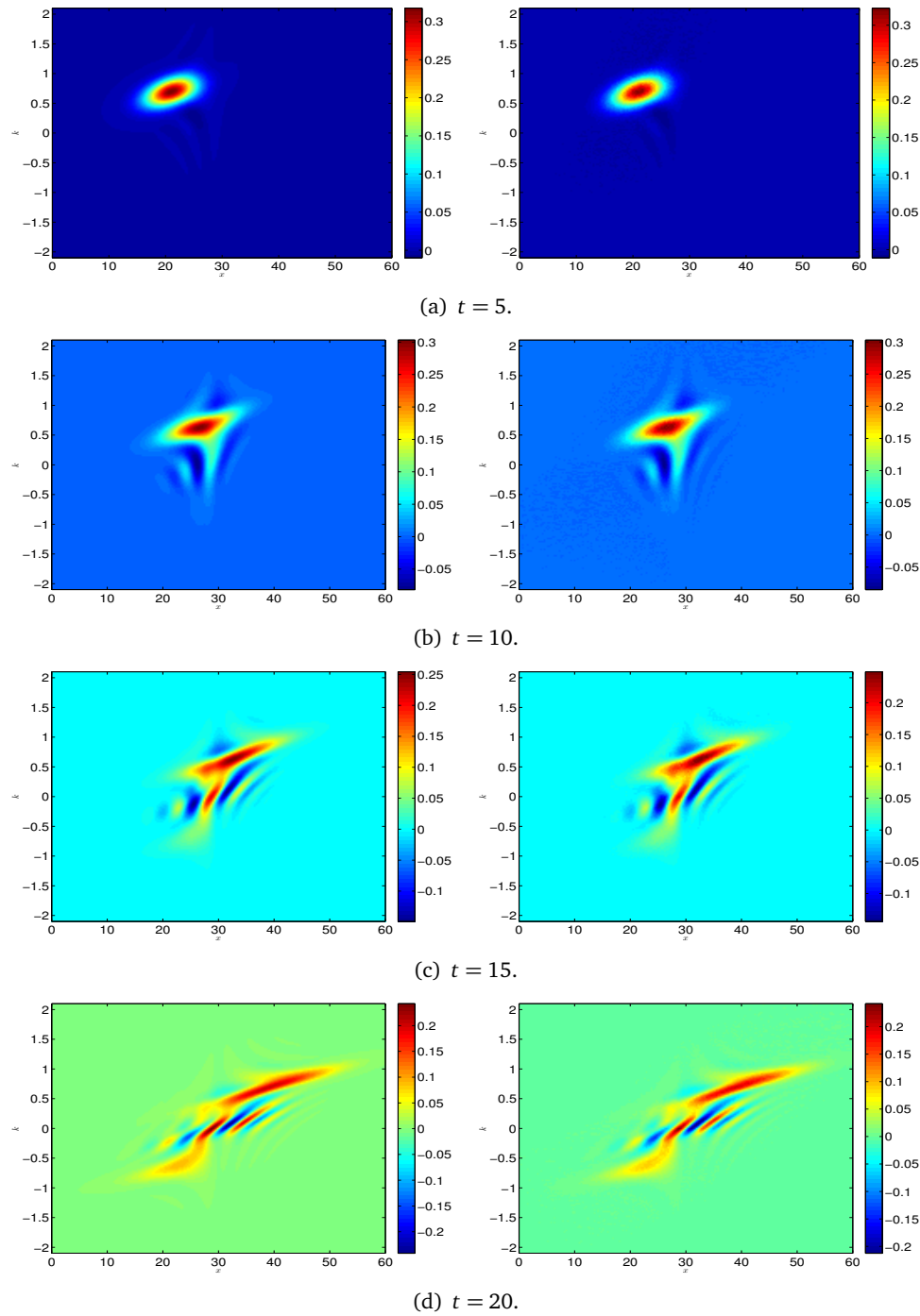


Figure 3: Partial reflection by the Gaussian barrier: Numerical Wigner functions at different time instants $t = 5, 20, 15, 20$ fs. The reference solution by SEM is displayed in the left-hand-side column, while the right-hand-side column shows the numerical solution obtained by wpWBRW with the auxiliary function $\gamma(x) = 3\xi^2$ as well as $\Delta t = 1$ fs and $T_A = 1$ fs.

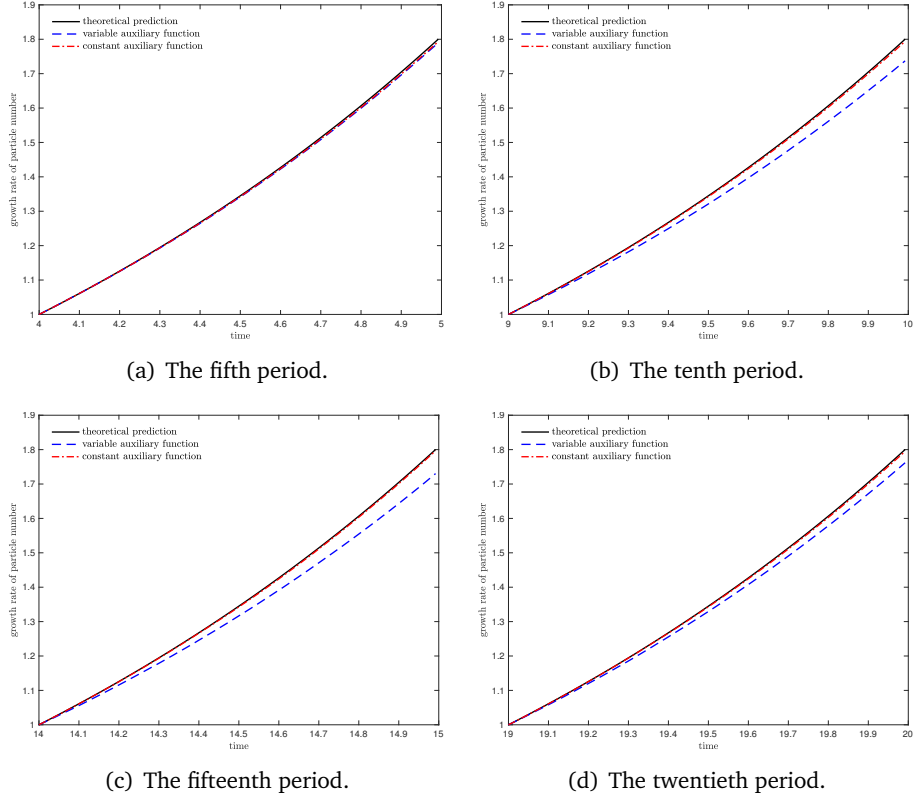


Figure 4: Partial reflection by the Gaussian barrier: Growth rates of particle number within different annihilation periods for wpWBRW with $\Delta t = 0.008\text{fs}$ and $T_A = 1\text{fs}$. The curve of theoretical prediction can be described analytically by $\Phi^{2\gamma_0 t}$ when using a constant auxiliary function γ_0 . Here we set the constant auxiliary function $\gamma_0 = \xi$ and the variable one $\gamma(x) = \xi(x)$.

In order to output the quantum observable $\langle \hat{A} \rangle$, e.g., the Wigner functions and the marginal distributions, at different instants, we adopt an equidistant partition of the time interval $[0, t_{fin}]$

$$0 = t_0 \leq t_1 \leq t_2 \leq \dots \leq t_{n-1} \leq t_n = t_{fin}, \quad t_{j+1} - t_j = \Delta t,$$

and evolve wpWBRW for n steps. Once wpWBRW starts, the number of particles increases exponentially with time, then necessary annihilation operations are required to ensure the simulation to continue. In this work, we perform these annihilation operations at a constant frequency, say $1/T_A$. That is, we divide equally the time interval $[0, t_{fin}]$ into n_A subintervals with the partition being

$$0 = t^0 < t^1 < t^2 < \dots < t^{n_A} = t_{fin}, \quad n_A = t_{fin}/T_A$$

with $\{t^l\}_{l=1}^{n_A} \subset \{t_j\}_{j=1}^n$. The annihilations occur exactly at the time instant t^i for $1 \leq i \leq n_A - 1$, at which the particle number decreases significantly from $\#_p^b(t^i)$ to $\#_p^a(t^i)$, where $\#_p^b$ (resp. $\#_p^a$) represents the particle number before (resp. after) the annihilation.

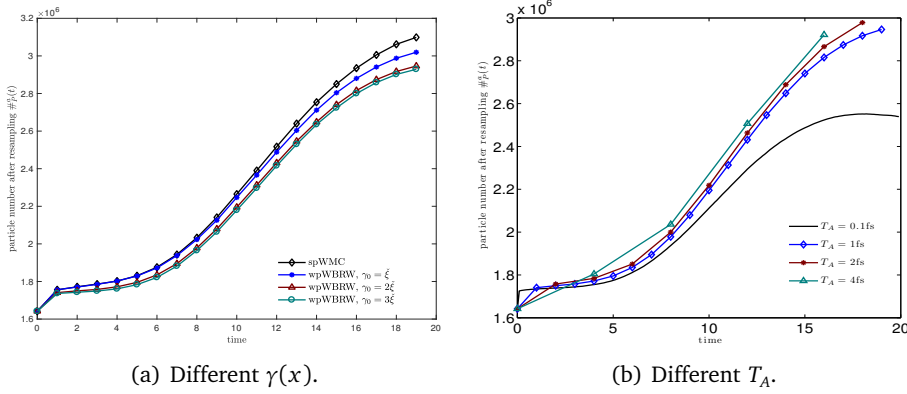


Figure 5: Partial reflection by the Gaussian barrier: Particle number after resampling (annihilation). The left plot shows the behavior for different auxiliary functions $\gamma(x)$ with the same annihilation period $T_A = 1$ fs. The right plot displays the behavior for different annihilation periods with the same constant auxiliary function $\gamma_0 = 2\xi$.

For convenience, we denote the particle number at t^0 and t^{n_A} by $\#_p^a(t^0)$ and $\#_p^b(t^{n_A})$, respectively. In each time period $[t^{i-1}, t^i]$, the particle number increases from $\#_p^a(t^{i-1})$ to $\#_p^b(t^i)$ and corresponding multiple is denoted by

$$M_i = \#_p^b(t^i) / \#_p^a(t^{i-1}). \quad (6.2)$$

For the k -truncated Wigner branching particle model with constant auxiliary function $\gamma(x) \equiv \gamma_0$, it has been proved in Theorem 5.5 that such increasing multiple only depends on the time increment T_A and γ_0 , which means the same increasing multiple exists for each time period, i.e., $M_i \equiv e^{2\gamma_0 T_A}$ for any $i \in \{1, 2, \dots, n_A\}$.

When the branching process evolves from $t_{j-1} = (j-1)\Delta t$ to $t_j = j\Delta t$ for $1 \leq j \leq n$, particle offspring will be generated. It should be emphasized here that, according to Theorem 5.6, the time step Δt does not matter in wpWBRW from the theoretical point view in the case of using a constant auxiliary function and whatever large or small Δt we choose the numerical results should be the same. Actually, there is no time discretization error for the weighted-particle implementation with a constant auxiliary function, see Eq. (7.9). The only reason we need the time steps is we want to output numerical results at the instant t_j . On the contrary, in the case of using a variable auxiliary function, like $\gamma(x) = \xi(x)$ in spWMC and $\gamma(x) = \xi(x)/2$ in RC, one must be very careful in choosing Δt , because, on one hand, Δt should be enough small due to the first-order time approximations (7.4) and (7.8), and on the other hand, too small time step significantly reduces the probability of branching, which is crucial to capture the quantum information in stochastic Wigner simulations [29]. This is another reason why we suggest the constant auxiliary function.

All the numerical results are obtained with our own Fortran implementations of wpWBRW, SEM and ASM on the computing platform: Dell Poweredge R820 with $4 \times$ Intel Xeon processor E5-4620 (2.2 GHz, 16 MB Cache, 7.2 GT/s QPI Speed, 8 Cores, 16 Threads) and 256GB memory.

6.1. 2D Gaussian barrier scattering

Two Gaussian barrier scattering experiments are conducted in 2D phase space. The first experiment is exactly the same as that adopted in [29], while the only change for the second one is the barrier height is increased to 1.3eV. The readers are referred to [29] for the details on the problem setting. As we pointed out earlier, both the k -truncated (see Eq. (3.1), the model parameter is Δy) and y -truncated (see Eq. (3.9), the model parameter is Δk) branching particle models can be regarded as approximations of the same Wigner equation in the unbounded domain, and thus comparable results are expected on the same footing because both Gaussian wavepacket and Gaussian barrier possess a very nice localized structure. Hence we only report numerical results for the k -truncated model and those for the y -truncated model can be found in [29] as well as in an early version of this work [33]. The initial particle number is fixed to be $\#_p^a(t^0) = 1641810$, and the reference solutions are obtained by SEM, the spectral accuracy of which was well demonstrated in [23, 29].

In general, the calculation of the normalizing function $\xi(x)$ in Eq. (5.3) and sampling from $V_W^+(x, k)/\xi(x)$ can be realized simultaneously, namely, we can calculate the normalization factor through sampling. The Gaussian barrier potential reads

$$V(x) = H_B \exp \left[-\frac{(x - x_B)^2}{2} \right], \quad (6.3)$$

where H_B and x_B denote the barrier height and the barrier center, respectively, and the explicit expression of corresponding Wigner kernel is

$$V_W(x, k) = \frac{2H_B}{\hbar} \sqrt{\frac{2}{\pi}} e^{-2k^2} \sin(2k(x - x_B)). \quad (6.4)$$

It can be easily seen here that $\sqrt{\frac{2}{\pi}} e^{-2k^2}$ in Eq. (6.4) is the probability density of the normal distribution $\mathcal{N}(0, 1/2)$, with which we can calculate the integral by the rejection sampling. In actual simulations, the number of samples are chosen as 2×10^8 for each x , and the numerical $\xi(x)$ is shown in Fig. 6 for $H_B = 0.3\text{eV}$ and $x_B = 30\text{nm}$. We find there that the normalization factor has a sharp decrease around $x = 30$, whereas it is very flat outside the neighborhood of $x = 30$ (see Fig. 6).

Experiment 6.1. To be convenient for comparison, we first take the same experiment as utilized before in [29], in which the barrier height is set to be $H = 0.3\text{eV}$ so that the Gaussian wavepacket will be partially reflected. Such partial reflection is clearly shown in Fig. 3. Five groups of tests with different time steps and annihilation frequencies are performed and related data are displayed in Table 1, from which we are able to find several observations below concerning the accuracy.

- (1) The idea of choosing constant auxiliary function $\gamma(x) \equiv \gamma_0$ works very well. As we expected, with the same Δt and T_A , the larger value γ_0 takes, the more accurate solution we obtain, which clearly manifests the reduction in variance.

Table 1: Partial reflection by the Gaussian barrier: Numerical data for wpWBRW and spWMC. The errors in the third, fourth and fifth columns are calculated at the final time $t_{fin} = 20\text{fs}$. The particle numbers in the sixth and seventh columns are measured in million. While using the constant auxiliary function $\gamma(x) \equiv \gamma_0$, the increasing multiple of particle number within an annihilation period is $e^{2\gamma_0 T_A}$. Three kinds of constant auxiliary functions, $\gamma_0 = \xi, 2\xi, 3\xi$, are tested, where $\xi = \max_{x \in \mathcal{X}} \{\xi(x)\} \approx 2.96\text{E-}01$.

Method	$\gamma(x)$	err_{wf}	err_{sm}	err_{mm}	$\#_p^b$	$\#_p^a$	M	$e^{2\gamma_0 T_A}$
$\Delta t = 0.008\text{fs}, T_A = 1\text{fs}$								
spWMC	$\xi(x)$	9.15E-02	3.30E-02	3.19E-02	5.33	3.03	1.77	–
wpWBRW	ξ	9.01E-02	3.16E-02	3.05E-02	5.44	3.02	1.80	1.81
	2ξ	7.95E-02	2.74E-02	2.46E-02	9.62	2.95	3.26	3.27
	3ξ	7.51E-02	2.52E-02	1.97E-02	17.25	2.93	5.89	5.91
$\Delta t = 1\text{fs}, T_A = 1\text{fs}$								
spWMC	$\xi(x)$	1.60E-01	1.17E-01	1.40E-01	5.49	3.13	1.77	–
wpWBRW	ξ	8.98E-02	3.32E-02	2.73E-02	5.44	3.02	1.80	1.81
	2ξ	7.94E-02	2.68E-02	2.21E-02	9.61	2.95	3.26	3.27
	3ξ	7.55E-02	2.51E-02	1.99E-02	17.26	2.93	5.89	5.91
$\Delta t = 2\text{fs}, T_A = 2\text{fs}$								
spWMC	$\xi(x)$	2.00E-01	1.48E-01	2.01E-01	9.86	3.26	3.12	–
wpWBRW	ξ	9.00E-02	3.45E-02	3.43E-02	10.07	3.10	3.25	3.27
	2ξ	6.32E-02	2.70E-02	2.36E-02	31.62	2.98	10.62	10.68
	3ξ	5.48E-02	2.45E-02	2.30E-02	102.25	2.94	34.71	34.88
$\Delta t = 4\text{fs}, T_A = 4\text{fs}$								
spWMC	$\xi(x)$	2.47E-01	1.66E-01	2.36E-01	30.07	3.48	9.72	–
wpWBRW	ξ	1.27E-01	4.93E-02	4.74E-02	33.19	3.21	10.46	10.68
	2ξ	6.69E-02	2.83E-02	2.79E-02	326.99	2.92	112.65	113.98
$\Delta t = 0.1\text{fs}, T_A = 0.1\text{fs}$								
spWMC	$\xi(x)$	2.86E-01	8.12E-02	6.82E-02	2.73	2.58	1.06	–
wpWBRW	ξ	2.87E-01	8.02E-02	6.53E-02	2.73	2.57	1.06	1.06
	2ξ	2.84E-01	8.01E-02	6.61E-02	2.87	2.55	1.13	1.13
	3ξ	2.84E-01	8.10E-02	6.60E-02	3.04	2.55	1.19	1.19

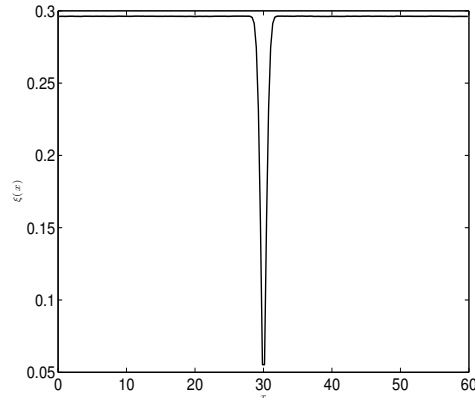


Figure 6: The normalizing function $\xi(x)$ for the Gaussian barrier (6.3) with $H_B = 0.3\text{eV}$ and $x_B = 30\text{nm}$ is utilized in the k -truncated Wigner simulations.

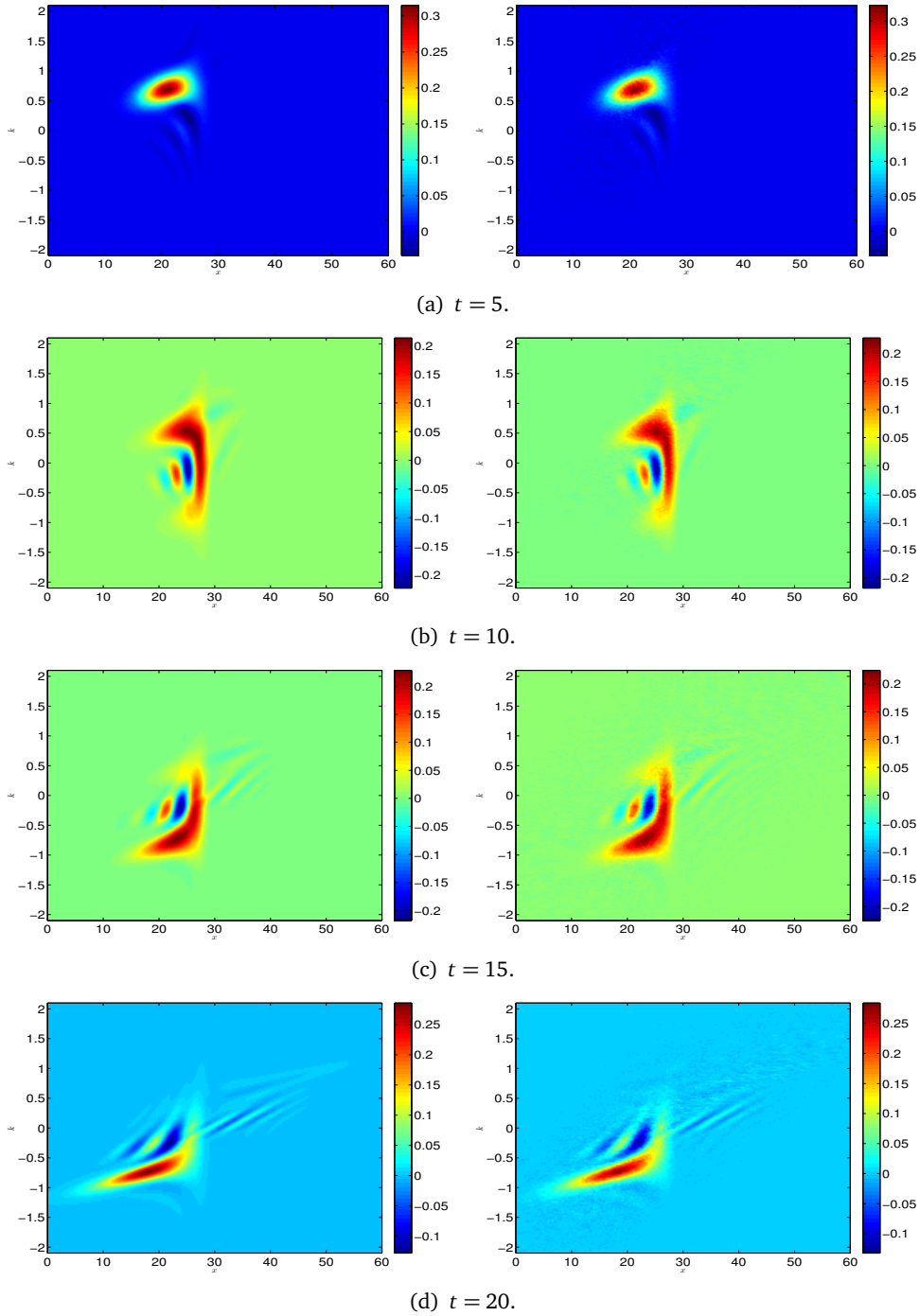


Figure 7: Total reflection by the Gaussian barrier: Numerical Wigner functions at different time instants $t = 5, 20, 15, 20$ fs. The reference solution by SEM is displayed in the left-hand-side column, while the right-hand-side column shows the numerical solution obtained by wpWBRW with the auxiliary function $\gamma(x) = 2\check{\xi}$ as well as $\Delta t = 1$ fs and $T_A = 1$ fs.

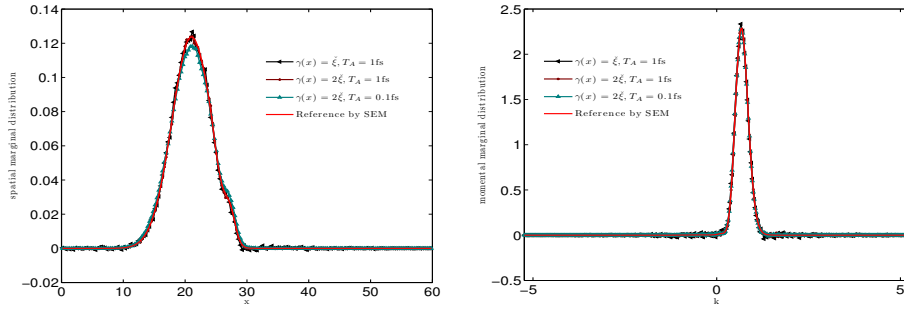
- (2) When the time step Δt is small, say $\Delta t = 0.008\text{fs}$ and 0.1fs , the accuracy of spWMC is comparable to that of wpWBRW with $\gamma(x) \equiv \check{\xi}$ under the same T_A , but the former becomes worse once Δt increases, like $\Delta t = 1\text{fs}$, 2fs and 4fs . The larger Δt gets, the worse the accuracy of spWMC becomes. On the contrary, the accuracy of wpWBRW is barely affected by the choice of Δt . While using the same annihilation frequency, say $T_A = 1\text{fs}$, smaller time step, e.g., $\Delta t = 0.008\text{fs}$, cannot improve the accuracy, as predicted by Theorem 5.6. In fact, the accuracy with $\Delta t = 0.008\text{fs}$ is almost identical to that with $\Delta t = 1\text{fs}$. Such observation directly reflects the fact that there is no time discretization errors in wpWBRW with a constant auxiliary function. A detailed discussion on this time discretization issue can be found in the end of this paper.
- (3) Highly frequent annihilation operations, e.g., $T_A = 0.1\text{fs}$, destroy the accuracy, even larger constant auxiliary function cannot save it. But this does not mean a low annihilation frequency should be appreciated. Actually, when using $T_A = 4\text{fs}$, the accuracy becomes worse than that using $T_A = 1\text{fs}$ or 2fs , which may be due to the accumulated numerical errors, such as the bias caused by the resampling. That is, as we mentioned before, the annihilation adopted here is nothing but a kind of resampling according to the histogram, and thus possibly cause some random noises due to its discontinuous nature.

Next we focus on the efficiency. One of the main variables shaping the efficiency is the particle number. Since the same initial particle distribution is employed for all runs, we only need to consider the growth rate of particle number. Once choosing the constant auxiliary function γ_0 and the annihilation frequency $1/T_A$, the increasing multiple of particle number can be exactly determined by $e^{2\gamma_0 T_A}$ from Theorem 5.5, and the ninth column of Table 1 shows corresponding theoretical predictions. In our numerical simulations, within every annihilation period $[t^{i-1}, t^i]$ with $1 \leq i \leq n_A$, we record the starting particle number $\#_p^a(t^{i-1})$, the ending particle number $\#_p^b(t^i)$, and the related growth rate M_i in Eq. (6.2). Let

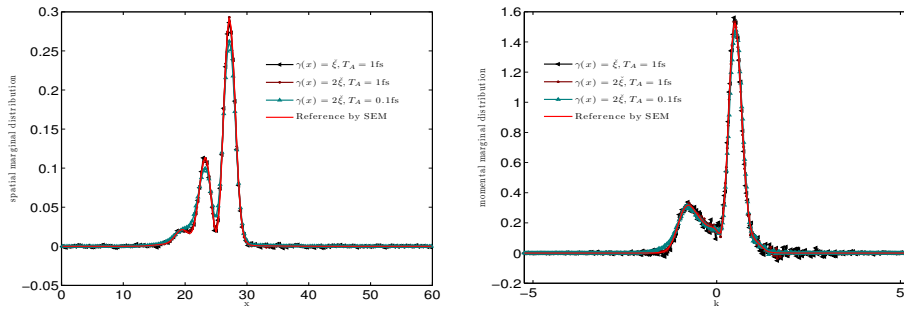
$$\check{\#}_p^a = \max_{0 \leq i \leq n_A - 1} \{\#_p^a(t^i)\}, \quad \check{\#}_p^b = \max_{1 \leq i \leq n_A} \{\#_p^b(t^i)\}, \quad \bar{M} = \frac{1}{n_A} \sum_{i=1}^{n_A} M_i.$$

Table 1 gives numerical values of above three quantities, see the sixth, seventh and eighth columns. According to Table 1, we can figure out the following facts on the efficiency.

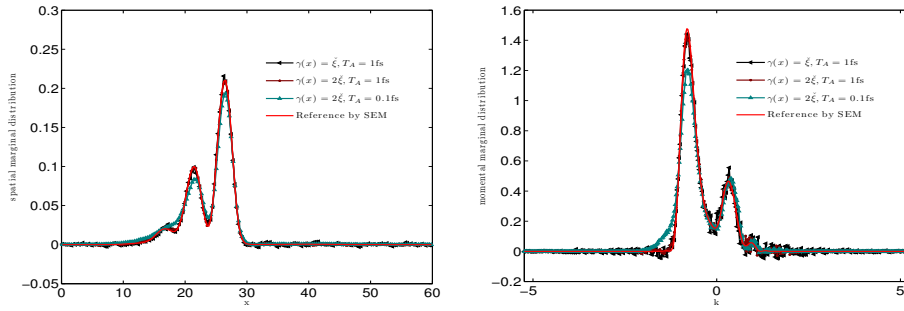
- (1) Agreement between the mean value \bar{M} and the theoretical prediction $e^{2\gamma_0 T_A}$ is readily seen in all situations. In this case, the average acceptance ratio α_0 almost equals to one due to the localized structure of the Wigner kernel (6.4). Actually, the growth rates in the first five annihilation periods, e.g. for $T_A = 1\text{fs}$ and $\gamma_0 = 3\check{\xi}$, are 5.92, 5.87, 5.88, 5.89, and 5.88, all of which are almost identical to the mean value of 5.89. When $T_A = 1, 2, 4\text{fs}$, the former is a little less than the latter, because the particles moving outside the computational domain $\mathcal{X} \times \mathcal{X}$ are not taken into account. Within each annihilation period, the maximum travel distance of particles can be



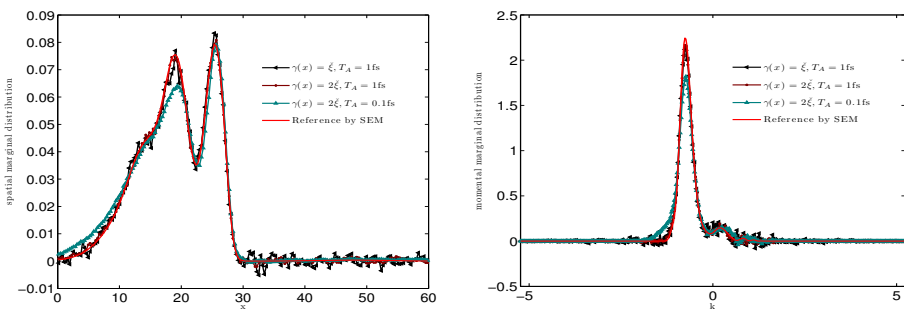
(a) $t = 5$.



(b) $t = 10$.



(c) $t = 15$.



(d) $t = 20$.

Figure 8: Total reflection by the Gaussian barrier: Spatial (left column) and momental (right) marginal probability distributions at $t = 5, 10, 15, 20$ fs.

Table 2: Total reflection by the Gaussian barrier: Numerical data for wpWBRW and spWMC. Detailed explanations are referred to Table 1, except for $\check{\xi} \approx 1.28$ here.

Method	$\gamma(x)$	err_{wf}	err_{sm}	err_{mm}	$\#_p^b$	$\#_p^a$	\overline{M}	$\mathbb{E}^{2\gamma_0 T_A}$
$\Delta t = 1\text{fs}, T_A = 1\text{fs}$								
spWMC	$\xi(x)$	2.6033E-01	6.8583E-02	9.3721E-02	48.72	3.95	12.46	-
wpWBRW	$\check{\xi}$	2.5998E-01	6.7069E-02	8.4044E-02	49.58	3.94	12.71	13.04
	$2\check{\xi}$	1.3034E-01	3.1041E-02	5.5122E-02	479.96	2.87	167.36	170.12
$\Delta t = 0.1\text{fs}, T_A = 0.1\text{fs}$								
spWMC	$\xi(x)$	3.4177E-01	1.1303E-01	1.9719E-01	3.22	2.50	1.29	-
wpWBRW	$\check{\xi}$	3.4201E-01	1.0674E-01	1.9785E-01	3.23	2.50	1.29	1.29
	$2\check{\xi}$	3.3697E-01	1.0959E-01	1.9413E-01	4.05	2.43	1.67	1.67
	$3\check{\xi}$	3.4011E-01	1.1157E-01	1.9734E-01	5.18	2.40	2.16	2.16

calculated by

$$\frac{\hbar}{m} \cdot \max_{k \in \mathcal{X}} \{|k|\} \cdot T_A,$$

implying that, the larger value T_A is, the more particles move outside the domain. This explains the slight deviation between \overline{M} and $\mathbb{E}^{2\gamma_0 T_A}$ increases from almost zero to at most 1.33 as T_A increases from 0.1fs to 4fs. Moreover, when $T_A = 1\text{fs}$, the increasing multiples for $\Delta t = 0.008\text{fs}$ are identical to those for $\Delta t = 1\text{fs}$, i.e., \overline{M} is independent of Δt , which has been also already predicted by the theoretical analysis. More details about the agreement of the growth rates of particle number with the theoretical prediction for $T_A = 1\text{fs}$ and $\Delta t = 0.008\text{fs}$ can be found in Fig. 4.

- (2) Not like using the constant auxiliary function, we do not have a simple calculation formula so far for the growth rate of particle number when using the variable auxiliary function (i.e., depending both on time and trajectories) in spWMC. However, we can still utilize the growth rate for the case of $\gamma_0 = \check{\xi}$ to provide a close upper bound for the case of $\gamma(x) = \xi(x)$. As shown in the eighth column of Table 1, the variation of the mean growth rate between them is about 0, 0.03, 0.13 and 0.74 for $T_A = 0.1\text{fs}$, 1fs, 2fs and 4fs, respectively. Fig. 4 further compares the curves of growth rate for $T_A = 1\text{fs}$ and $\Delta t = 0.008\text{fs}$ within four typical annihilation periods. By comparing with the Wigner functions shown in Fig. 3, we find that the closer to the center the Gaussian wavepacket lives, the larger the deviation between the curves for the constant and variable auxiliary functions becomes. Such deviation in accordance with the analysis of $\xi(x)$ shown in Fig. 6 validates the proposed mathematical theory again.
- (3) During the resampling (annihilation) procedure, the main objective is to reconstruct the Wigner distribution using less particles, which explores the cancelation of the weights with opposite signs, see Eq. (5.47). The eighth column of Table 1 tells us that the maximum particle numbers after resampling for $T_A = 1, 2, 4\text{fs}$ are all around 3.00 million, implying that there should be a minimal requirement of particle number to achieve a comparable accuracy. Otherwise, the accuracy will decrease, for example,

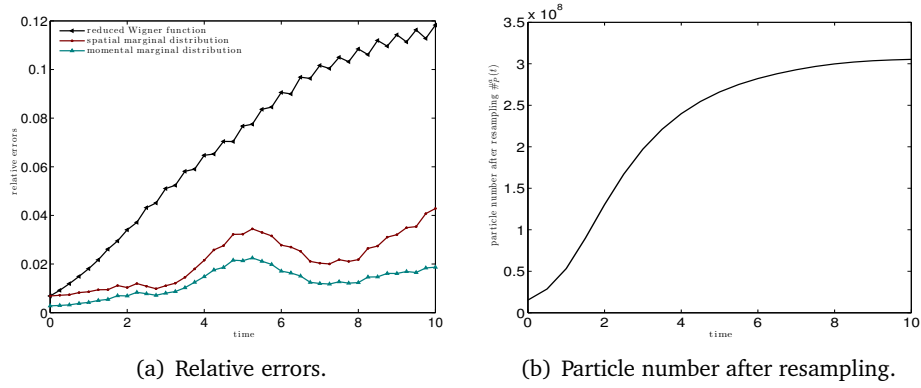


Figure 9: The Helium-like system: The history of relative errors and particle number after resampling.

the values of $\#_p^a$ for $T_A = 0.1\text{fs}$ are around 2.55 million. Fig. 5 shows more clearly the typical history of $\#_p^a(t)$. We can find there that, no matter how huge the particle number before the annihilation $\#_p^b(t)$ (which depends on the choice of both the auxiliary function and T_A) is, the particle number after the annihilation $\#_p^a(t)$ for the simulations with comparable accuracy exhibits almost the same behavior, which recovers and extends the so-called “bottom line” structure described in [29]. Such behavior may depend only on the oscillating structure of the Wigner function. On the other hand, highly frequent annihilations like $T_A = 0.1\text{fs}$ destroy this bottom line structure and thus the accuracy, see Fig. 5(b), implying that there are not enough particles to capture the oscillating nature.

Experiment 6.2. In this example, we increase the barrier height to $H = 1.3\text{eV}$ so that the Gaussian wavepacket will be totally reflected, see Fig. 7. Such augment of the barrier height implies that the growth rate of particle number now is about $1.3/0.3 \approx 4.33$ times larger than that for Experiment 1, and thus it is more difficult to simulate accurately. Based on the observations in Experiment 1, we only test two groups of annihilation periods, $T_A = 0.1, 1\text{fs}$. Table 2 summarizes the running data and confirms again that, the larger constant auxiliary function improves the accuracy, whereas the higher annihilation frequency destroys the accuracy. In order to get a more clear picture on this accuracy issue, we plot both spatial and momental probability distributions at different time instants $t = 5, 10, 15, 20\text{fs}$ in Fig. 8 against the reference solutions by SEM. We can easily see there that, the loss of accuracy when using $T_A = 0.1\text{fs}$ is mainly due to that there are not enough generated particles to capture the peaks reflecting off the barrier; while the increase of accuracy when using a larger constant auxiliary function, e.g., $\gamma_0 = 2\check{\xi}$, comes from the smaller variation. Actually, similar phenomena also occur in Experiment 1.

6.2. A 4D Helium-like system

As a typical example, a one-dimensional two-body Helium-like system has been considered in testing deterministic Wigner solvers in 4D phase space [24]. Here we adopt the

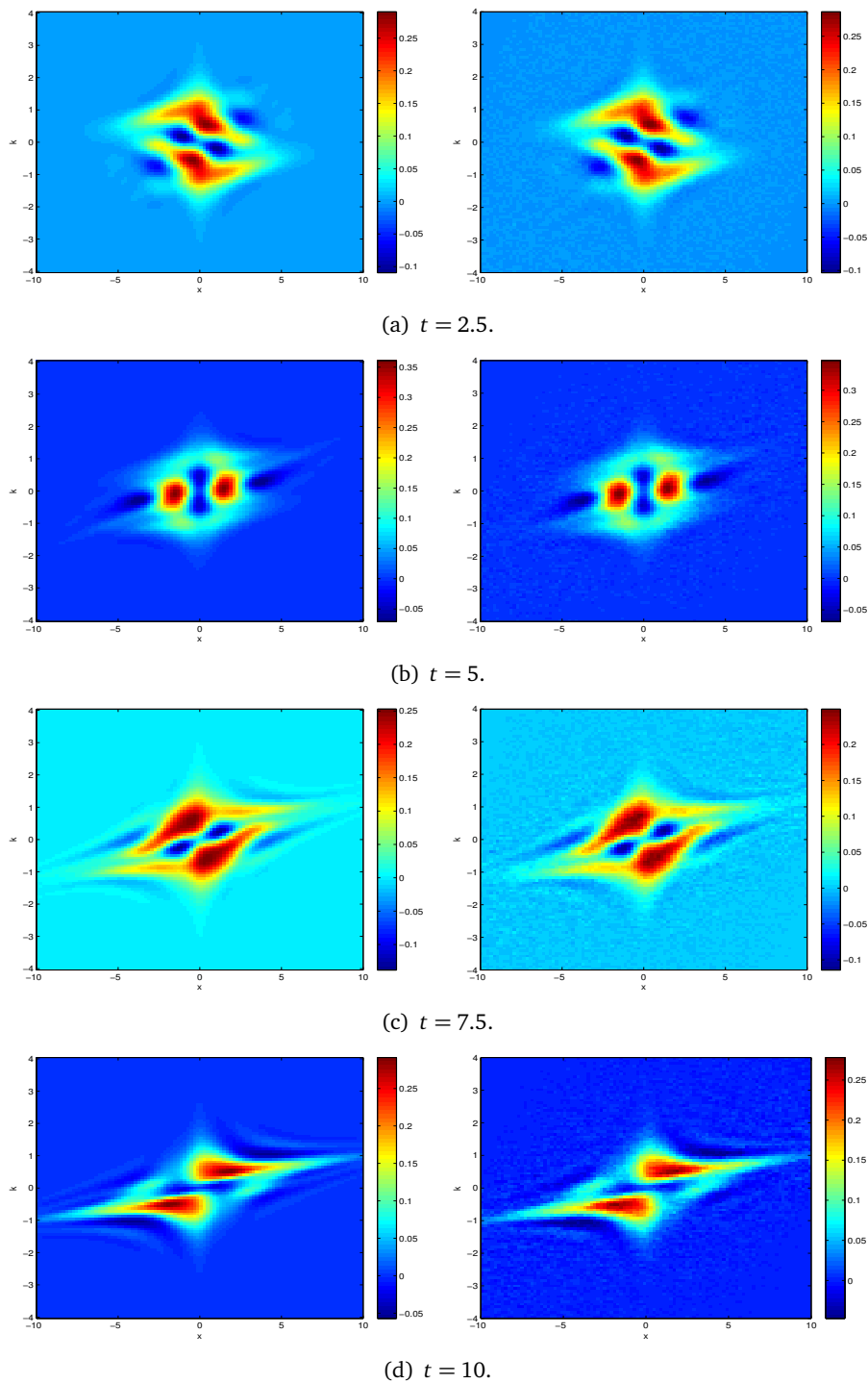


Figure 10: The Helium-like system: Numerical reduced Wigner functions at $t = 2.5, 5, 7.5, 10$. The left column displays the reference solution by ASM, while the right column shows the numerical solution by wWBRW with the constant auxiliary function $\gamma_0 = 2$, $\Delta t = 0.25$ and $T_A = 0.5$.

potential:

$$V(x_1, x_2) = V_{ne}(x_1) + V_{ne}(x_2) + V_{ee}(x_1, x_2) = -\frac{2e^{-\kappa|x_1-x_A|}}{2\kappa} - \frac{2e^{-\kappa|x_2-x_A|}}{2\kappa} + \frac{e^{-\kappa|x_1-x_2|}}{2\kappa},$$

which is composed of the electron-nucleus and electron-electron interactions, where κ expresses the screening strength, x_A denotes the position of the nucleus, and $x_i (i = 1, 2)$ is the position of the i -th electron. In fact, $e^{-\kappa|x_1-x_2|}/2\kappa$ is Green's function of the 1D screened Poisson equation. The Wigner kernel of the electron-nucleus interaction reads

$$V_{W,ne}(x_i, k_i) = -\frac{2}{\hbar\pi} \cdot \frac{\sin(2(x_i - x_A))}{4k_i^2 + \kappa^2}, \quad i = 1, 2,$$

and that of the electron-electron interaction

$$V_{W,ee}(x_1, x_2, k_1, k_2) = \frac{1}{\hbar\pi} \cdot \frac{\sin(2k_1x_1 + 2k_2x_2)}{|k_1 - k_2|^2 + \kappa^2} \cdot \delta(k_1 + k_2).$$

Therefore we can use a simple rejection method to draw samples from the target distribution $V_W^+(x, k)/\xi(x)$. Here we use the atomic unit, set $x_A = 0$ and $\kappa = 0.5$ and adopt the same initial data as used in [24]. The computational domain $\mathcal{X} \times \mathcal{K} = [-10, 10]^2 \times [-4, 4]^2$ is divided into 100^4 cells. The reference solution is obtained by ASM on a uniform grid mesh with $\Delta t = 0.05$ and $\Delta x_1 = \Delta x_2 = 0.2$, while the \mathcal{K} -domain is divided into 8 cells and each cell contains 16 collocation points, and the \mathcal{Y} -domain is $[-22.5, 22.5]^2$.

To monitor the accuracy, we record the relative errors of the reduced single-body Wigner function as given in [24], and of corresponding marginal probability distributions. Fig. 9(a) shows the history of those relative errors. We can see there that, although the reduced Wigner function is comparatively less accurate, it can still yield a more accurate estimation of macroscopically measurable quantities, such as the spatial and momental marginal probability distributions. This also explains why we see more noise in Fig. 10 for the reduced Wigner function than in Fig. 11 for the marginal distributions. The possible reason may lie on the fact that if we wish to be able to estimate a function with the same accuracy as a function in low dimensions, then we need the size of samples to grow exponentially as well. However, it can be readily observed in Figs. 10 and 11 that the main features captured by wpWBRW are almost identical to those by ASM.

Finally, we would like to mention that the growth of particle number is closely related to the number of cells (dimensionality of feature space). In this example, we use a $100^4 = 10^8$ uniformly distributed cells for the resampling and set the initial particle number to be about 1.5×10^7 with the total weighted summation being 1×10^7 . It is shown in Fig. 9(b) that the particle number increases soon to 3×10^8 , which is comparable to the cell number, and then approaches a stable value around 3.1×10^8 . So if we refine those cells for the resampling, then the particle number will increase to a higher level. Actually, for higher-dimensional problems like $d \geq 3$, the number of cells is much higher than that of samples and such a simple cell based resampling strategy cannot achieve an efficient annihilation. Hence we have to resort to other advanced techniques to control the sample size in higher-dimensional phase space.

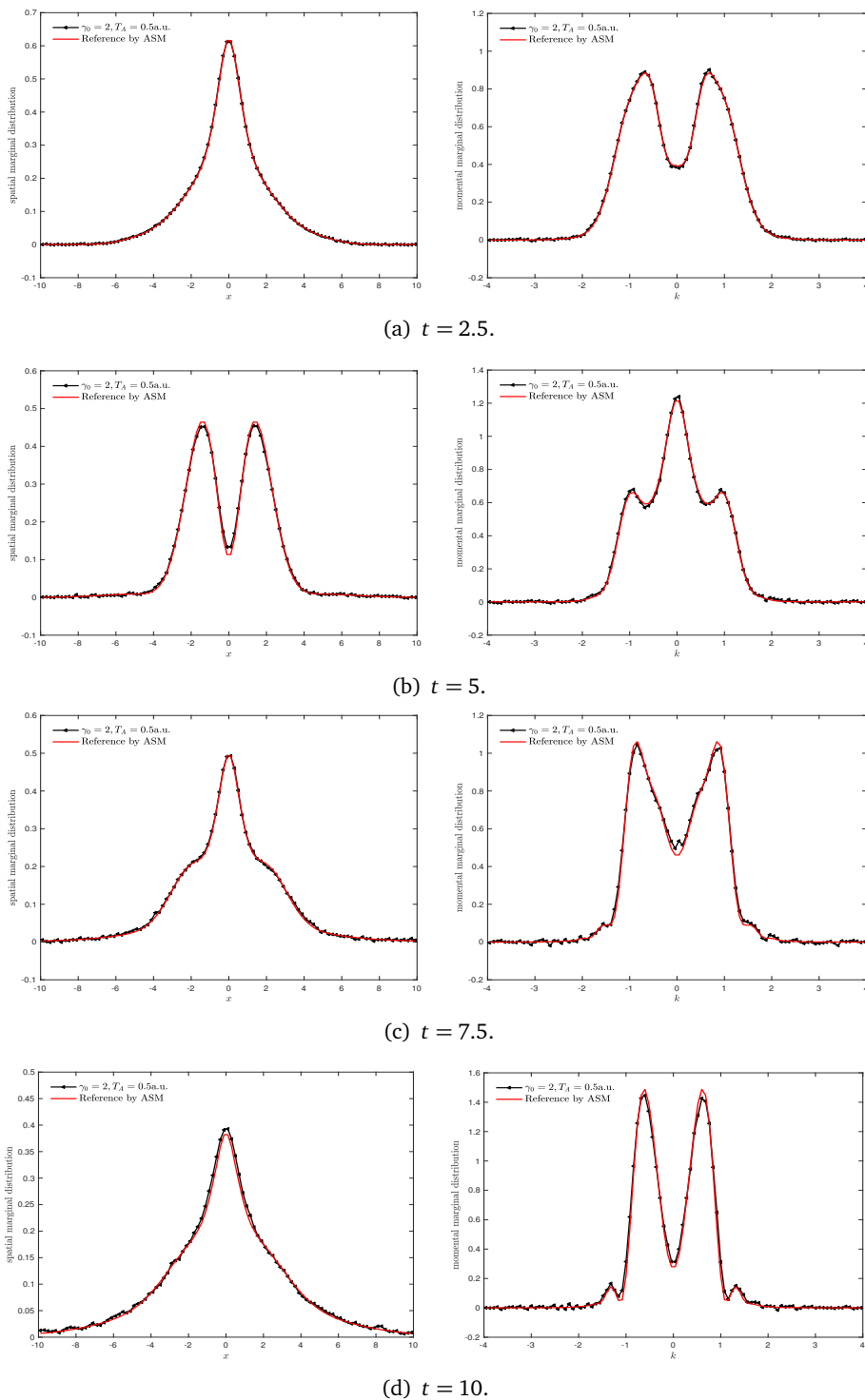


Figure 11: The Helium-like system: Spatial (left column) and momental (right column) marginal probability distributions at $t = 2.5, 5, 7.5, 10$.

7. Conclusions and discussion

This paper is devoted to the mathematical foundation of the branching random walk algorithm for the many-body Wigner quantum dynamics. Although several concepts, such as the signed particle, the adjoint equation and the annihilation procedure, have already been mentioned in previous work, unfortunately related mathematical results are somewhat fragmented or lack of systemic elaboration, and the crucial issues, such as the annihilation of particles and the computational complexity, fall outside the scope of any current available theory. Thus, our contribution is to provide a framework from the viewpoint of computational mathematics within which all these problems can be fully addressed, and interested readers may get a complete view of the weighted-particle Wigner branching random walk (wpWBRW) algorithm accompanied with both derivation and implementation details in a single reference. Only by this way can we analyze its accuracy, point out the numerical challenge and make further improvements. We have shown that the signed particle is naturally introduced according to the principle of importance sampling, the motion of particles is described by a probabilistic model, and the annihilation is nothing but the re-sampling. Actually, a direct iterative treatment of the renewal-type integral equation leads to the description based on the Neumann series for the signed-particle Wigner Monte Carlo (spWMC) algorithm [28], but this series form may be not so rigorous because of possible convergence issues. Moreover, we adopt a different approach from that shown recently in the random cloud (RC) algorithm [32], while both approaches succeed in validating the basis of the spWMC. The reason we prefer to the branching random walk model, a mixture of the branching process and the random walk, is that the theory of branching process not only provides a natural interpretation of growth of particles, but also allows us to calculate the particle growth rate exactly and discuss the conservation property. These results are extremely important in real simulations since it gives us a reasonable criterion to control the computational complexity and allocate computational resources efficiently.

More importantly, the freedom in choosing the auxiliary function are fully revealed here and the resulting wpWBRW algorithm shows a nice feature of variance reduction by increasing the constant auxiliary function. This property is absent in other existing implementations such as spWMC and RC. We will give a rigorous proof of such variance reduction in a forthcoming publication. Besides this, wpWBRW with a constant auxiliary function has no time discretization errors. This can be verified from another point on the life-length τ and the time step Δt , which is worthy of being paid attention to, but easily being ignored. The life-length of each particle, initially at time t_0 , satisfies

$$\tau \propto \left. \frac{d\mathcal{G}(t'; \mathbf{r}, t_0)}{dt'} \right|_{t'=t_0+\tau}. \quad (7.1)$$

To draw samples from such a distribution, we can draw a uniform random number u in $[0, 1)$ such that

$$u = \mathcal{G}(t_0 + \tau; \mathbf{r}, t_0), \quad (7.2)$$

and then a simple calculation yields

$$-\ln(1-u) = \int_{t_0}^{t_0+\tau} \gamma(\mathbf{r}(s-t_0)) ds. \quad (7.3)$$

However, solving Eq. (7.3) for τ is entirely not trivial as the explicit form of $\gamma(\mathbf{x})$ is unknown. The spWMC algorithm uses an approximation like [27, 28]

$$\gamma(\mathbf{r}(s-t_0)) \approx \gamma(\mathbf{r}), \quad (7.4)$$

and thus

$$\tau \approx \tilde{\tau} = -\frac{\ln(1-u)}{\gamma(\mathbf{r})}. \quad (7.5)$$

The approximate life-length $\tilde{\tau}$ depends on the state of particle, and the approximation (7.4) is usually reasonable when $\gamma(\mathbf{r}) = \xi(\mathbf{r})$ is very flat. But, for example, around the neighborhood of $x = 30\text{nm}$ as shown in Fig. 6, such approximation may be too rough to be used and will give rise to additional numerical errors. This can be exactly quantified through a simple fact:

$$\begin{aligned} \frac{d\mathcal{G}(t'; \mathbf{r}, t_0)}{dt'} &= \gamma(\mathbf{r}) e^{-\gamma(\mathbf{r})(t'-t_0)} \cdot \frac{\gamma(\mathbf{r}(t'-t_0)) e^{-\int_{t_0}^{t'} \gamma(\mathbf{r}(s-t_0)) ds}}{\gamma(\mathbf{r}) e^{-\gamma(\mathbf{r})(t'-t_0)}} \\ &= \frac{d\tilde{\mathcal{G}}(t'; \mathbf{r}, t_0)}{dt'} \cdot \eta(\mathbf{r}, t'-t_0), \end{aligned} \quad (7.6)$$

where

$$\frac{d\tilde{\mathcal{G}}(t'; \mathbf{r}, t_0)}{dt'} = \gamma(\mathbf{r}) e^{-\gamma(\mathbf{r})(t'-t_0)}, \quad \eta(\mathbf{r}, \tau) = \frac{\gamma(\mathbf{r}(\tau))}{\gamma(\mathbf{r})} \cdot e^{-\int_{t_0}^{t_0+\tau} [\gamma(\mathbf{r}(s-t_0)) - \gamma(\mathbf{r})] ds}.$$

Therefore, the above approximation (7.4) equals to taking $\tilde{\mathcal{G}}(t'; \mathbf{r}, t_0)$ as the instrumental exponential distribution, yielding

$$\tilde{\tau} \propto \left. \frac{d\tilde{\mathcal{G}}(t'; \mathbf{r}, t_0)}{dt'} \right|_{t'=t_0+\tau}. \quad (7.7)$$

That is, spWMC ignores completely the bias introduced by $\eta(\mathbf{r}, \tau)$, and thus puts a severe limitation on the time step Δt , as $\eta(\mathbf{r}, \tau) \approx 1$ is only valid when $\tau \leq \Delta t \ll 1$ [29]. A similar story happens to the RC algorithm [30, 32], in which $\gamma(\mathbf{r}) = \xi(\mathbf{r})/2$ is chosen and it is suggested to use the following first-order approximation

$$\Pr(\tau > \Delta t) = 1 - G(t_0 + \Delta t; \mathbf{r}, t_0) = e^{-\int_{t_0}^{t_0+\Delta t} \gamma(\mathbf{r}(s-t_0)) ds} \approx 1 - \gamma(\mathbf{r})\Delta t + \mathcal{O}(\Delta t^2). \quad (7.8)$$

When Δt is sufficiently small, $\gamma(\mathbf{r})\Delta t$ can be treated as the probability of the branching-and-jump event. However, such approach still introduces additional errors and poses formidable restriction on Δt when $\gamma(\mathbf{r})$ is very large. By contrast, when choosing the

constant auxiliary function $\gamma(\mathbf{r}) \equiv \gamma_0$, the life-length τ of each particle is exactly determined only by γ_0 as

$$\tau = -\frac{\ln(1-u)}{\gamma_0}, \quad (7.9)$$

which has nothing to do with the state of particle in contrast to $\tilde{\tau}$ in Eq. (7.5), and the constant auxiliary function directly leads to $\eta(\mathbf{r}, \tau) \equiv 1$, thereby getting rid of the bias. This is the first reason why we say that there is no time discretization error in the wpWBRW method with the constant auxiliary function. The second one is the direct inference of Theorem 5.6, implying that whatever large or small Δt we choose, it does not produce any impact on the expectation of the total particle number of the branching process with a constant auxiliary function. Hence the importance of the flexibility on the choice of a constant auxiliary function cannot be over-exaggerated.

Acknowledgments This research was supported by grants from the National Natural Science Foundation of China (Nos. 11471025, 11421101, 11822102). Y. X. is partially supported by The Elite Program of Computational and Applied Mathematics for PhD Candidates in Peking University. The authors are grateful to the useful discussions with Zhenzhu Chen, Paul Ellinghaus, Mihail Nedjalkov and Jean Michel Sellier on the signed particle Monte Carlo method for the y -truncated Wigner equation.

References

- [1] J. L. DOOB, *Classical Potential Theory and Its Probabilistic Counterpart*, Springer-Verlag, Berlin, reprint edition, 2001.
- [2] E. B. DYNKIN, *Diffusions, Superdiffusions and Partial Differential Equations*, American Mathematical Society, 2002.
- [3] M. NEDJALOV AND P. VITANOV, *Application of the iteration approach to the ensemble Monte Carlo technique*, *Solid-State Electron*, 33 (1990), pp. 407–410.
- [4] H. KOSINA, M. NEDJALOV AND S. SELBERHERR, *Theory of the Monte Carlo method for semiconductor device simulation*, *IEEE Trans. Electron Devices*, 47 (2000), pp. 1898–1908.
- [5] H. KOSINA, M. NEDJALOV AND S. SELBERHERR, *The stationary Monte Carlo method for device simulation, I, Theory*, *J. Appl. Phys.*, 93 (2003), pp. 3553–3563.
- [6] M. NEDJALOV, H. KOSINA AND S. SELBERHERR, *The stationary Monte Carlo method for device simulation, II, Event biasing and variance estimation*, *J. Appl. Phys.*, 93 (2003), pp. 3564–3571.
- [7] C. YAN, W. CAI AND X. ZENG, *A parallel method for solving Laplace equations with Dirichlet data using local boundary integral equations and random walks*, *SIAM J. Sci. Comput.*, 35 (2013), pp. B868–B889.
- [8] I. KOSZTIN, B. FABER AND K. SCHULTEN, *Introduction to the diffusion Monte Carlo method*, *Am. J. Phys.*, 64 (1996), pp. 633–643.
- [9] M. HAIRER AND J. WEARE, *Improved diffusion Monte Carlo*, *Commun. Pure Appl. Math.*, 67 (2014), pp. 1995–2021.
- [10] E. WIGNER, *On the quantum corrections for thermodynamic equilibrium*, *Phys. Rev.*, 40 (1932), pp. 749–759.

- [11] V. I. TATARSKIĬ, *The Wigner representation of quantum mechanics*, Sov. Phys. Usp, 26 (1983), pp. 311–327.
- [12] W. H. ZUREK, *Decoherence and the transition from quantum to classical*, Phys. Today, 44 (1991), pp. 36–44.
- [13] C. JACOBONI AND P. BORDONE, *The Wigner-function approach to non-equilibrium electron transport*, Rep. Prog. Phys., 67 (2004), pp. 1033–1071.
- [14] N. C. DIAS AND J. N. PRATA, *Admissible states in quantum phase space*, Ann. Phys., 313 (2004), pp. 110–146.
- [15] P. A. MARKOWICH, C. A. RINGHOFER AND C. SCHMEISER, *Semiconductor Equations*, Springer-Verlag, Wien-New York, 1990.
- [16] B. A. BIEGEL, *Quantum Electronic Device Simulation*, PhD thesis, Stanford University, 1997.
- [17] R. BALESCU, *Equilibrium and Nonequilibrium Statistical Mechanics*, John Wiley & Sons, New York, 1975.
- [18] W. P. SCHLEICH, *Quantum Optics in Phase Space*, Wiley-VCH, Berlin, 2011.
- [19] J. M. SELLIER, M. NEDJALOV AND I. DIMOV, *An introduction to applied quantum mechanics in the Wigner Monte Carlo formalism*, Phys. Rep., 577 (2015), pp. 1–34.
- [20] U. LEONHARDT, *Measuring the Quantum State of Light*, Cambridge University Press, New York, 1997.
- [21] D. LEIBFRIED, T. PFAU AND C. MONROE, *Shadows and mirrors: Reconstructing quantum states of atom motion*, Phys. Today, 1988, pp. 22–28.
- [22] C. ZACHOS, *Deformation quantization: quantum mechanics lives and works in phase-space*, Int. J. Mod. Phys. A, 17 (2002), pp. 297–316.
- [23] S. SHAO, T. LU AND W. CAI, *Adaptive conservative cell average spectral element methods for transient Wigner equation in quantum transport*, Commun. Comput. Phys., 9 (2011), pp. 711–739.
- [24] Y. XIONG, Z. CHEN AND S. SHAO, *An advective-spectral-mixed method for time-dependent many-body Wigner simulations*, SIAM J. Sci. Comput., 38 (2016), pp. B491–B520.
- [25] D. QUERLIOZ AND P. DOLLFUS, *The Wigner Monte Carlo Method for Nanoelectronic Devices: A Particle Description of Quantum Transport and Decoherence*, Wiley-ISTE, London, 2010.
- [26] M. NEDJALOV, H. KOSINA, S. SELBERHERR, C. RINGHOFER AND D. K. FERRY, *Unified particle approach to Wigner-Boltzmann transport in small semiconductor devices*, Phys. Rev. B, 70 (2004), 115319.
- [27] M. NEDJALOV, P. SCHWAHA, S. SELBERHERR, J. M. SELLIER AND D. VASILESKA, *Wigner quasi-particle attributes – An asymptotic perspective*, Appl. Phys. Lett., 102 (2013), 163113.
- [28] J. M. SELLIER, M. NEDJALOV, I. DIMOV AND S. SELBERHERR, *A benchmark study of the Wigner Monte-Carlo method*, Monte Carlo Methods Appl., 20 (2014), pp. 43–51.
- [29] S. SHAO AND J. M. SELLIER, *Comparison of deterministic and stochastic methods for time-dependent Wigner simulations*, J. Comput. Phys., 300 (2015), pp. 167–185.
- [30] O. MUSCATO AND W. WAGNER, *A class of stochastic algorithms for the Wigner equation*, SIAM J. Sci. Comput., 38 (2016), pp. A1483–A1507.
- [31] P. ELLINGHAUS, *Two-Dimensional Wigner Monte Carlo Simulation for Time-Resolved Quantum Transport with Scattering*, PhD thesis, Institute for Microelectronics, TU Vienna, 2016.
- [32] W. WAGNER, *A random cloud model for the Wigner equation*, Kinet. Relat. Mod., 9 (2016), pp. 217–235.
- [33] S. SHAO AND Y. XIONG, *A computable branching process for the Wigner quantum dynamics*, arXiv:1603.00159v1, 2016.
- [34] J. S. LIU, *Monte Carlo Strategies in Scientific Computing*, Springer, New York, 2001.
- [35] T. E. HARRIS, *The Theory of Branching Processes*, Springer-Verlag, Berlin, 1963.

- [36] H. JIANG, W. CAI AND R. TSU, *Accuracy of the Frenselly inflow boundary condition for Wigner equations in simulating resonant tunneling diodes*, J. Comput. Phys., 230 (2011), pp. 2031–2044.
- [37] A. ARNOLD, H. LANGE AND P. F. ZWEIFEL, *A discrete-velocity, stationary Wigner equation*, J. Math. Phys., 41 (2000), pp. 7167–7180.
- [38] T. GOUDON, *Analysis of a semidiscrete version of the Wigner equation*, SIAM J. Numer. Anal., 40 (2002), pp. 2007–2025.
- [39] T. GOUDON AND S. LOHRENGEL, *On a discrete model for quantum transport in semi-conductor devices*, Transport Theory Statist. Phys., 31 (2002), pp. 471–490.
- [40] A. PAZY, *Semigroups of Linear Operators and Applications to Partial Differential Equations*. Springer-Verlag, New York, 1983.
- [41] O. KALLENBERG, *Foundations of Modern Probability*, Springer, New York, 2nd Ed., 2002.
- [42] R. KRESS, *Linear Integral Equations*, Springer, New York, 3rd Ed., 2014.
- [43] T. HASTIE, R. TIBSHIRANI AND J. FRIEDMAN, *The Elements of Statistical Learning: Data Mining, Inference, and Prediction*, Springer, New York, 2nd Ed., 2009.
- [44] A. DOUCET, N. DE FREITAS AND N. GORDON, *An Introduction to Sequential Monte Carlo Methods. Sequential Monte Carlo Methods in Practice*, Springer-Verlag, New York, 2001.
- [45] H. KOSINA, M. NEDJALKOV AND S. SELBERHERR, *Solution of the space-dependent Wigner equation using a particle model*, Monte Carlo Methods Appl., 10 (2004), pp. 359–368.
- [46] Y. XIONG AND S. SHAO, *The Wigner branching random walk: Efficient implementation and performance evaluation*, Commun. Comput. Phys., (2018), In press (arXiv:1709.02121).
- [47] S. RJASANOW AND W. WAGNER, *A stochastic weighted particle method for the Boltzmann equation*, J. Comput. Phys., 124 (1996), pp. 243–253.
- [48] B. YAN AND R. E. CAFLISCH, *A Monte Carlo method with negative particles for Coulomb collisions*, J. Comput. Phys., 298 (2015), pp. 711–740.
- [49] C. P. ROBERT AND G. CASELLA, *Monte Carlo Statistical Methods*, Springer, New York, 2nd Ed., 2004.